NAVAL POSTGRADUATE SCHOOL
Monterey, California

THESIS

DESIGN OF DIGITAL CONTROL ALGORITHMS FOR
UNMANNED AIR VEHICLES

by

Steven J. Froncillo

March 1998

Thesis Advisor: Isaac. I. Kaminer

Approved for public release; distribution is unlimited.

REPORT DOCUMENTATION PAGE

Form Approved
OMB No. 0704-0188

Public reporting burden for this collection of information is estimated to average 1 hour per response, including the time for reviewing instruction, searching existing data sources, gathering and maintaining the data needed, and completing and reviewing the collection of information. Send comments regarding this burden estimate or any other aspect of this collection of information, including suggestions for reducing this burden, to Washington headquarters Services, Directorate for Information Operations and Reports, 1215 Jefferson Davis Highway, Suite 1204, Arlington, VA 22202-4302, and to the Office of Management and Budget, Paperwork Reduction Project (0704-0188) Washington DC 20503.

1. AGENCY USE ONLY (Leave blank)	2. REPORT DATE March 1998	3. REPORT TYPE AND DATES COVERED Master's Thesis

4. TITLE AND SUBTITLE DESIGN OF DIGITAL CONTROL ALGORITHMS FOR UNMANNED AIR VEHICLES	5. FUNDING NUMBERS
6. AUTHOR(S) Froncillo, Steven J.	

7. PERFORMING ORGANIZATION NAME(S) AND ADDRESS(ES) Naval Postgraduate School Monterey, CA 93943-5000	8. PERFORMING ORGANIZATION REPORT NUMBER

9. SPONSORING / MONITORING AGENCY NAME(S) AND ADDRESS(ES)	10. SPONSORING / MONITORING AGENCY REPORT NUMBER

11. SUPPLEMENTARY NOTES

The views expressed in this thesis are those of the author and do not reflect the official policy or position of the Department of Defense or the U.S. Government.

12a. DISTRIBUTION / AVAILABILITY STATEMENT Approved for public release; distribution is unlimited.	12b. DISTRIBUTION CODE

13. ABSTRACT (maximum 200 words)

Recent advances in the design of high performance aircraft, such as fly-by-wire controls, complex autopilot systems, and unstable platforms for greater maneuverability, are all possible due to the use of digital control systems. With the aid of modern control tools and techniques based on state-space methods, the aerospace engineer has the ability to design a dynamic aircraft model, verify its accuracy, and design and implement the controller within a matter of a few months. This work examines the digital control design process utilizing a Rapid Prototyping System developed at the Naval Postgraduate School. The entire design process is presented, from design of the controller to implementation and flight test on an Unmanned Air Vehicle (UAV).

14. SUBJECT TERMS Unmanned Aerial Vehicles, Rapid Prototyping Systems, Hardware-In-The-Loop Simulation, AROD, FROG, MATRIXx, SystemBuild	15. NUMBER OF PAGES 100
	16. PRICE CODE

17. SECURITY CLASSIFICATION OF REPORT Unclassified	18. SECURITY CLASSIFICATION OF THIS PAGE Unclassified	19. SECURITY CLASSIFI- CATION OF ABSTRACT Unclassified	20. LIMITATION OF ABSTRACT UL

Approved for public release; distribution is unlimited

DESIGN OF DIGITAL CONTROL ALGORITHMS FOR UNMANNED AIR VEHICLES

Steven J. Froncillo
Lieutenant Commander, United States Navy
B.S., University of Rhode Island, 1983

Submitted in partial fulfillment of the
requirements for the degree of

MASTER OF SCIENCE IN AERONAUTICAL ENGINEERING

from the

NAVAL POSTGRADUATE SCHOOL
March 1998

ABSTRACT

Recent advances in the design of high performance aircraft, such as fly-by-wire controls, complex autopilot systems, and unstable platforms for greater maneuverability, are all possible due to the use of digital control systems. With the aid of modern control tools and techniques based on state-space methods, the aerospace engineer has the ability to design a dynamic aircraft model, verify its accuracy, and design and implement the controller within a matter of a few months. This work examines the digital control design process utilizing a Rapid Prototyping System developed at the Naval Postgraduate School. The entire design process is presented, from design of the controller to implementation and flight test on an Unmanned Air Vehicle (UAV).

TABLE OF CONTENTS

I.   INTRODUCTION

The use of digital computers in the real-time control of aircraft has paved the way to new aircraft designs that are faster, more maneuverable and safer than ever before. With this growing emphasis on digital control design, new tools and techniques have been developed to aid in the design and implementation of complex control systems. Traditionally, control systems are developed using classical control design methods that are costly and time consuming. Newer technologies, like rapid prototyping based on modern control methods, integrate the design process and shorten the time required to complete a control design from a few years to a few months.

The purpose of this thesis is twofold: develop the background material for an Advanced Control of Aerospace Vehicles course, and design and flight test an altitude hold controller for a UAV.

At the Naval Postgraduate School, students in the Aeronautical and Avionics Engineering curriculum receive a full sequence of controls courses with the final course being Advanced Control of Aerospace Vehicles, for which this thesis is written. This course will introduce the students to the critical aspects of the design, implementation and flight testing of the basic controllers for fixed-wing aircraft. The course examines both classical (transform) and modern (state-space) control methods for designing complex digital control systems.

The main focus is on the study of sampled-data systems, systems that have both discrete and continuous-time components. Devices used for the interface between the continuous and discrete components, the analog-to-digital converter and the digital-to-analog converter, are covered in detail. This thesis will derive mathematical models for each of these operations, and develop tools for analysis and synthesis.

The class is largely project oriented. Much of the class is concentrated in the Avionics/Controls laboratory and the Unmanned Air Vehicle (UAV) laboratory. The projects are centered on a Rapid Prototyping System (RPS) developed by the aeronautical engineering department for flight testing control algorithms for unmanned air vehicles. The system affords a small team the ability to test new concepts in guidance, navigation,

and digital control. The RPS consists of commercially available rapid prototyping software with an open architecture design to allow for a wide range of applications. The application software developed by Integrated Systems Incorporated (ISI), called RealSim, allows students to participate in design projects from the initial concept stage to the flight testing phase of the design process. This software has two main advantages:

- The ability to automatically generate higher-language code such as C for the designed controller.

- The system utilizes industry standard I/O devices including digital-to-analog, analog-to-digital, pulse width modulation, and serial capability, permitting easy connections to hardware.

The test bed aircraft used is a UAV called *FROG*, shown in Figure 1.1. This UAV is equipped with a complete avionics suite necessary for autonomous flight.

The accomplishment of this endeavor has led to a number of successful projects, including voice controlled flight and an airspeed controller, and is paving the way for more complex projects such as autonomous landing. This thesis will describe in detail one such design project, the development of an altitude hold controller implemented in the *FROG* using the RPS tools. The automation of the design process is completed in three developmental phases:

- Feedback controller design. In this phase a model of the plant is created. The controller is then designed through various methods of classical input/output control techniques and/or modern state-space control techniques. The process typically involves many iterations to satisfy specific design requirements.

- Hardware-In-the-Loop Testing. The feedback system is tested with some or all of the actual hardware which will be used to control the aircraft. This is the final validation of the controller prior to an actual flight.

2

- Implementation and Flight Test. The controller is implemented in the Fight Management System used to control the *FROG* and then flight tested.

The design process described above is completed entirely with the RealSim series rapid prototyping software and real-time control hardware integrated with the system.
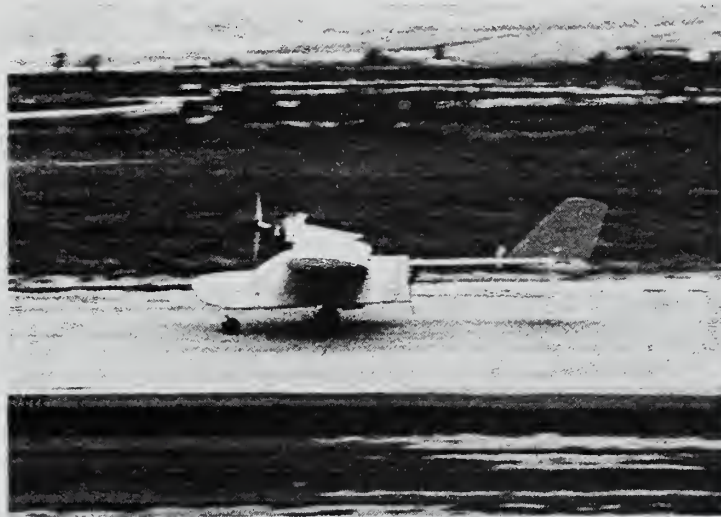

Figure 1.1: UAV *FROG*

II.   SAMPLED-DATA SYSTEMS

The systems and signals studied in the control of aerospace vehicles are referred to as sampled-data systems and have both discrete and continuous components, see Figure 2.1, where a continuous-time, or analog signal, is to be processed using a computer or special-purpose Digital Signal Processing (DSP) chip set. The interface between the continuous and discrete systems include the analog-to-digital (A/D) and the digital-to-analog (D/A) converters.
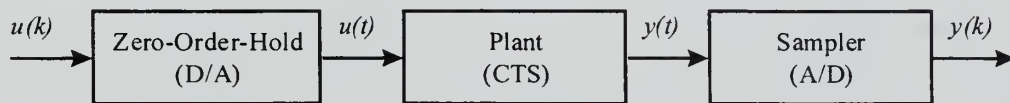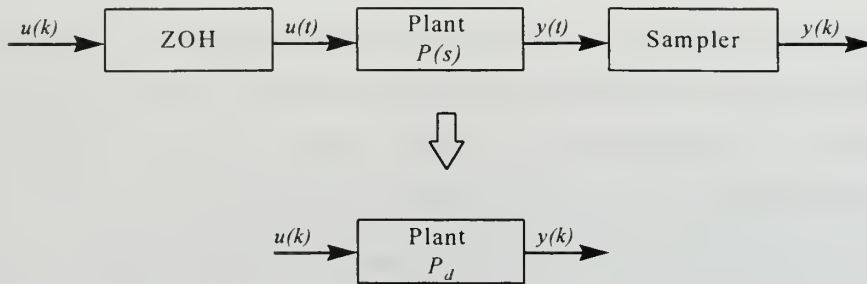

Figure 2.1: Sampled-Data System

The conversion of the a discrete to an analog signal by the D/A converter, which usually uses a Zero-Order-Hold (ZOH), involves scaling the digital values and converting them to a piecewise-constant continuous output. Where the conversion of the analog signal to a discrete sequence by the A/D converter is accomplished by a sample-and-hold circuit, called a Sampler.

This chapter will describe the operations of the digital-to-analog converter and analog-to-digital converter and methods for obtaining discrete models of continuous-time systems.   Material presented in this chapter is in the form of classroom notes, for further discussion refer to [Ref. 1,2,3].

A.   DISCRETE MODELS OF SAMPLED-DATA SYSTEMS

In this section we establish a general method for obtaining the difference equations that represent the behavior of the sampled-data system.   The resulting equivalent discrete system will then be analyzed using the sample-to-sample discrete

transfer function of a continuous system between a D/A and an A/D, as shown in Figure

2.2.

Where

$$P = \begin{cases} \dot{x} = A \cdot x + B \cdot u \\ y = C \cdot x + D \cdot u \end{cases}$$

$$P_d = \begin{cases} x_{k+1} = A_d \cdot x_k + B_d \cdot u_k \\ y_k = C_d \cdot x_k + D_d \cdot u_k \end{cases}$$

Figure 2.2: Equivalent Sampled-Data System

1.   Digital-to-Analog Converters (D/A)

Digital-to-analog converters usually use zero-order hold or (ZOH): given a sequence of samples, $u(kT)$ at $t = kT$, and holding its output constant at this value until the next sample is taken at $t = kT + T$ to produce a continuous signal. The piecewise constant output of the D/A is the signal $u(t)$ that is applied to the plant. Thus, the value of $u(t)$ consists of steps as seen in Figure 2.3.

6

2. Analog-to Digital Converters (A/D)

The analog-to-digital converter samples the analog signal $y(t)$ at discrete times and passes them to the computer. The time interval between samples y_k is called the sampling interval T. The A/D converter has two functions: quantizing the sampled analog signal into a discrete set of levels and coding the quantized representation into an acceptable format.
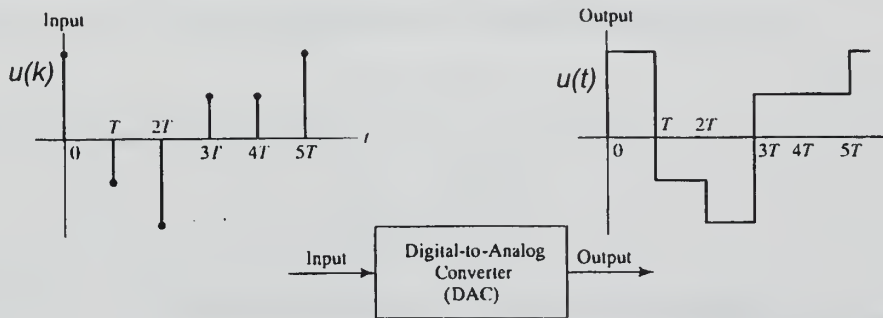

Figure 2.3: Digital-to-Analog Conversion

3. Discretization of Continuous-Time Systems

Consider a linear, continuous-time system

$$P = \begin{cases} \dot{x} = A \cdot x + B \cdot u \\ y = C \cdot x + D \cdot u \end{cases},$$

then

$$x(t) = e^{A(t-t_0)} \cdot x(t_0) + \int_{t_0}^{t} e^{A(t-\tau)} \cdot B \cdot u(\tau) \cdot d\tau .$$

To discretize let: $t_0 = kT$; $t = kT + T$ and assuming u is held constant over the sampling interval T (ZOH with no delay)

$$u(\tau) = u(kT) \quad ; \qquad [kT \le \tau < kT + T]$$

Then

$$x(kT + T) = e^{A(T)} \cdot x(kT) + \int_{kT}^{kT+T} e^{A(kT+T-\tau)} \cdot B \cdot u(\tau) \cdot d\tau$$

Let

$$\xi = (kT + T) - \tau$$

$$d\xi = -d\tau,$$

then

$$\tau = kt \Rightarrow \xi = T$$
$$\tau = kT + T \Rightarrow \xi = 0$$

Let $x(kT+T) = x_{k+1}$, then

$$x_{k+1} = e^{A \cdot T} \cdot x_k + \int_0^T e^{A \cdot \xi} \cdot B \cdot u_k \cdot d\xi \qquad \text{(Eq. 2.1)}$$

Define

$$\Phi = e^{AT}$$

$$\Gamma = \int_0^T e^{A\xi} \cdot B \cdot d\xi$$

The discrete equivalent of P

$$P_d = \begin{cases} x_{k+1} = \Phi \cdot x_k + \Gamma \cdot u_k \\ y_k = C \cdot x_k + D \cdot u_k \end{cases} \qquad \text{(Eq. 2.2)}$$

Note the equivalent discrete system is shift-invariant, since Φ and Γ are not functions of k. Commands to discretize: Matlab--c2d, Xmath--discretize

EXAMPLE 2.1:   Discretize the following CTS

$$\dot{x} = -a \cdot x + a \cdot u$$
$$y = x$$
$$\qquad P(s) = \frac{a}{s+a}$$

From equation 2.2

$$\Phi = e^{-a \cdot T}$$

$$\Gamma = \int_0^T e^{-a \cdot \xi} \cdot (a) \cdot d\xi = (1 - e^{-aT})$$

$$x_{k+1} = e^{-a \cdot T} \cdot x_k + (1 - e^{-a \cdot T}) \cdot u_k$$

$$y_k = x_k$$

8

B.   THE *Z*-TRANSFORM

1.   Definition

Given a sequence $\{x_k\}$, $k = -\infty, \ldots \infty$, let

$$X(z) = \sum_{k=-\infty}^{\infty} x_k \cdot z^{-k} , \qquad\qquad r_o < |z| < R_0 , \qquad\qquad \text{(Eq. 2.3)}$$

where we assume we can find values of r_o and for which the series converges.

As in the case of the Laplace transform, Eq. (2.3) is considered an operator that transforms a sequence x_k into a function $X(z)$, symbolically represented by

$$X(z) = Z\{x_k\}$$

The x_k and $X(z)$ are said to form a z-transform pair denoted as

$$X(z) \leftrightarrow Z\{x_k\}$$

EXAMPLE 2.2   Consider the sequence given in example problem 2.1

$$P(s) = \frac{a}{s+a} \qquad\Rightarrow\qquad x_k = e^{-akT} \qquad ; \qquad k=0,1,2,\ldots$$

By Eq. (2.3) the z-transform of x_k is

$$Z\{x_k\} = X(z) = \sum_{k=0}^{\infty} e^{-akT} z^{-k} = \sum_{k=0}^{\infty} (e^{-a \cdot T} \cdot z^{-1})^k$$

Note: a infinite geometric sum is given by

$$S_n = \sum_{m=0}^{\infty} \alpha^m = \frac{1}{1-\alpha} \qquad ; \qquad |\alpha| < 1$$

Letting $\alpha = (e^{-a \cdot T} \cdot z^{-1})$

$$X(z) = \frac{1}{1-(e^{-a \cdot T} \cdot z^{-1})} \quad ; \qquad \left| e^{-a \cdot T} \cdot z^{-1} \right| < 1 \quad ; \quad |z| > e^{-aT}$$

2.   Some Properties of the z-Transform

Listed below are some properties of the z-transform useful to the material presented in this section. For reference, a more complete list is found in [Ref. 1].

Linearity: given $\{x_k\}$, $\{y_k\}$

$$Z(x_k + y_k) = Z(x_k) + Z(y_k)$$

$$Z[\,a\,(x_k + y_k)] = Z(a\,x_k) + Z(a\,y_k) = a\,X(z) + a\,Y(z) \quad ; \quad \text{where } a = \text{constant}$$

Time Shifting:

$$Z\{x(k \pm n)\} = z^{\pm n}\,X(z)$$

Gives transform pairs

$$x(k+1) \leftrightarrow z\,X(z)$$

$$x(k-1) \leftrightarrow z^{-1}\,X(z)$$

Demonstrated by

$$Z(x_{k+1}) = z(x_k)$$

$$Z(x_{k+1}) = \sum_{0}^{\infty} x_{k+1} \cdot z^{-k} = \sum_{0}^{\infty} x_{k+1} \cdot z^{-k-1+1}$$

$$= \sum_{0}^{\infty} x_{k+1} \cdot z^{-(k+1)} \cdot z$$

$$= z \cdot X(z)$$

Final Value Theorem:

$$\lim_{k \to \infty} x(k) = \lim_{z \to 1} (z-1) X(z)$$

if such limits exists.

EXAMPLE 2.3: Find the z-transform given in example problem 2.1.

$$Z\left\{ \begin{array}{l} x_{k+1} = e^{-aT} \cdot x_k + (1 - e^{-aT}) u_k \\ y_k = x_k \end{array} \right\}$$

$$\left. \begin{array}{l} zX(z) = e^{-aT} \cdot X(z) + (1 - e^{-aT}) \cdot U(z) \\ Y(z) = X(z) \end{array} \right\} \Rightarrow \frac{Y(z)}{U(z)} = \frac{1 - e^{-aT}}{z - e^{-aT}}$$

C. ANALYSIS OF DISCRETE-TIME SYSTEMS

1. The Discrete Transfer Function

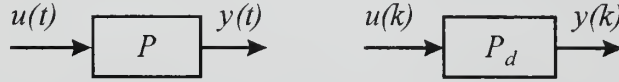Consider the continuous-time and discrete-time systems shown in Figure 2.4.

Figure 2.4: System Transfer Functions

The transfer function for the continuous-time system is

$$Y(s) = \left\{ C(sI - A)^{-1} \cdot B + D \right\} \cdot U(s)$$

For the discrete-time system compute

$$Z \begin{cases} x_{k+1} = \Phi \cdot x_k + \Gamma \cdot u_k \\ y_k = C \cdot x_k + D \cdot u_k \end{cases}$$

$$Z(x_{k+1}) = Z(\Phi \cdot x_k + \Gamma \cdot u)$$
$$z \cdot X(z) = \Phi \cdot X(z) + \cdot \Gamma \cdot U(z)$$

$$X(z) = (zI - \Phi)^{-1} \cdot \Gamma \cdot U(z)$$

$$Z(y_k) = Z(C \cdot x_k + D \cdot u_k)$$
$$Y(z) = C \cdot X(z) + D \cdot U(z)$$

$$Y(z) = \underbrace{\left\{ C \cdot (zI - \Phi)^{-1} \cdot \Gamma + D \right\}}_{T_d} \cdot U(z)$$

Discrete transfer function

$$\frac{Y(z)}{U(z)} = C \cdot (zI - \Phi)^{-1} \cdot \Gamma + D \qquad \text{(Eq. 2.4)}$$

EXAMPLE 2.4: Find the discrete transfer function from example problem 2.1

Given:

$$P(s) = \frac{a}{s + a}$$

Continuous-Time

$$Y(s) = [C \cdot (sI - A)^{-1} \cdot B + D] \cdot U(s) \Rightarrow Y(s) = \frac{a}{s + a} \cdot U(s)$$

Discrete-Time

$$\Phi = e^{-a \cdot T} \qquad \Gamma = \int_0^T e^{-a \cdot \xi} \cdot (a) d\xi = (1 - e^{-aT})$$

From Eq. (2.4)

$$\frac{Y(z)}{U(z)} = (1)[zI - e^{-a \cdot T}]^{-1} \cdot (1 - e^{-aT}) = \frac{1 - e^{-aT}}{z - e^{-a \cdot T}}$$
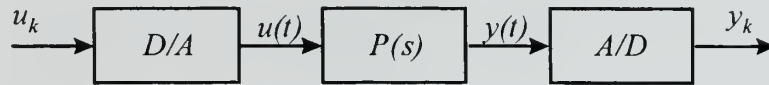
Now consider the sampled-data system in Figure 2.5.

Figure 2.5: Prototype Sampled-Data System

Let

$$u(kT) = \begin{cases} 1; k = 0 \\ 0; k \neq 0 \end{cases}$$

Then *u(k)* is the unit impulse. The response to a unit impulse determines the impulse response of the D/A converter:

$$u(t) = 1(t) - 1(t - T)$$

Then

$$U(s) = \frac{1}{s} - \frac{e^{-sT}}{s} = \frac{1}{s}\left(1 - e^{-sT}\right)$$

and

$$y(t) = L^{-1}\left(\frac{G(s)}{s} \cdot \left(1 - e^{-sT}\right)\right)$$

$$y(kT) = y(t), \quad (k-1)T \leq t \leq kT$$

12

Finally,

$$G(z) = Z(y(kT))$$

$$= Z\left\{ L^{-1}\left(\frac{G(s)}{s} \cdot \left(1 - e^{-sT}\right) \right) \right\}$$

$$= (1 - z^{-1}) \cdot Z\left\{ L^{-1}\left(\frac{G(s)}{s} \right) \right\}$$

$$= (1 - z^{-1}) \cdot Z\left(\frac{G(s)}{s} \right) \qquad \text{(Eq. 2.5)}$$

Where the "L^{-1}" is dropped for convenience.

EXAMPLE 2.5: Compute the discrete transfer function for

$$G(s) = \frac{a}{s + a}$$

Then

$$\frac{G(s)}{s} = \frac{1}{s} - \frac{1}{s + a}$$

The corresponding time function

$$L^{-1}\left\{ \frac{G(s)}{s} \right\} = 1(t) - e^{-a}(t)$$

$$y(kT) = 1(kT) - e^{-akT} \cdot 1(kT)$$

The z transform

$$Z\left\{ \frac{G(s)}{s} \right\} = Z(y(kT)) = \frac{z}{z-1} - \frac{z}{z - e^{-at}} = \frac{z(1 - e^{-aT})}{(z-1)(z - e^{-aT})}$$

From equation 2.5

$$G(z) = (1 - z^{-1})\left\{ \frac{z(1 - e^{-aT})}{(z-1)(z - e^{aT})} \right\}$$

$$= \frac{1 - e^{-aT}}{z - e^{-aT}}$$

The transfer function can also be obtained from the system's response to a unit pulse. Suppose the system input, u_k for $k > 0$, and the initial conditions are known, then writing out each term of the difference equation gives:

$$x_1 = \Phi \cdot x_0 + \Gamma \cdot u_0$$
$$x_2 = \Phi \cdot x_1 + \Gamma \cdot u_1 = \Phi \cdot (\Phi \cdot x_0 + \Gamma \cdot u_0) + \Gamma \cdot u_1 = \Phi^2 \cdot x_0 + \Phi \cdot \Gamma \cdot u_0 + \Gamma \cdot u_1$$
$$\vdots$$
$$x_k = \Phi^k \cdot x_0 + \Phi^{k-1} \cdot \Gamma \cdot u_0 + \Phi^{k-2} \cdot \Gamma \cdot u_1 + \ldots \Gamma \cdot u_{k-1}$$

Therefore,

$$x_k = \Phi^k \cdot x_0 + \sum_{i=0}^{k-1} \Phi^{k-i} \cdot \Gamma \cdot u_i$$

$$y_k = C \cdot \Phi^k \cdot x_0 + \sum_{i=0}^{k-1} \underbrace{C \cdot \Phi^{k-i} \cdot \Gamma}_{h_d(k-i)} \cdot u_i$$

(Eq. 2.6)

Suppose $x_0 = 0$ and

$$u_k = \begin{cases} 1; k = 0 \\ 0; k \neq 0 \end{cases},$$

then

$$y_k = \sum_{i=0}^{k} h_d(k-i) \cdot u_i = h_d(k).$$

In general,

$$y_k = \sum_{k=-\infty}^{\infty} h_d(k-i) \cdot u_i.$$

2. Block Diagrams and State-Space Descriptions

The discrete transfer function, in the z-domain, represents a linear algebraic relationship, accordingly multiple linear systems may be described by a system of linear equations.

Parallel Connections: The system response of a parallel combination of two LTI systems is the sum of the single-path transfer function, Figure 2.6.
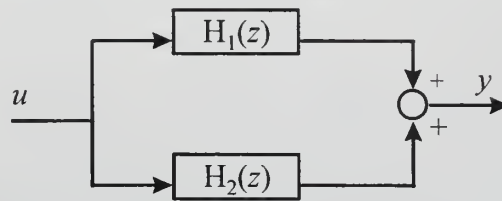

Figure 2. 6: Parallel blocks

$$Y(z) = \underbrace{[H_1(z) + H_2(z)]}_{H(z)} \cdot U(z) = H(z) \cdot U(z)$$

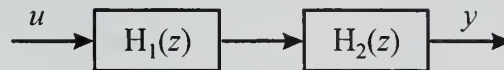**Cascade Connections:** The system response of two LTI systems in series is related by the product, Figure 2.7.

Figure 2.7: Cascade blocks

$$\left. \begin{array}{l} Y_1(z) = H_1(z) \cdot U(z) \\ Y(z) = H_2(z) \cdot Y_1(z) \end{array} \right\} Y(z) = H_1(z) \cdot H_2(z) \cdot U(z)$$

Feedback Connections: The transfer function of a single loop, Figure 2.8, is given by:
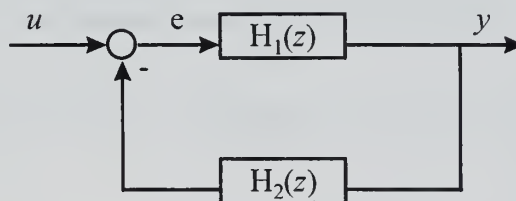

Figure 2. 8: Feedback transfer function

15

$$\left.\begin{array}{l} y = H_1 \cdot e \\ e = u - H_2 \cdot y \end{array}\right\} \Rightarrow y = H_1 \cdot (u - H_2 \cdot y) \Rightarrow Y(z) = \frac{H_1(z)}{1 + H_1(z) \cdot H_2(z)} \cdot U(z)$$

These transfer function relationships can be used in combination to describe complex multi-path systems.

In general

$$H(z) = \frac{a_0 + a_1 \cdot z^{-1} + \ldots a_m \cdot z^{-m}}{1 + b_1 \cdot z^{-1} + b_2 \cdot z^{-2} + \ldots b_n \cdot z^{-n}} = \frac{a(z)}{b(z)}$$

Example of 3rd order system

$$H(z) = \frac{a_1 \cdot z^{-1} + a_2 \cdot z^{-2} + a_3 \cdot z^{-3}}{1 + b_1 \cdot z^{-1} + b_2 \cdot z^{-2} + b_3 \cdot z^{-3}}$$

State-space realization (control canonical form), Figure 2.9.
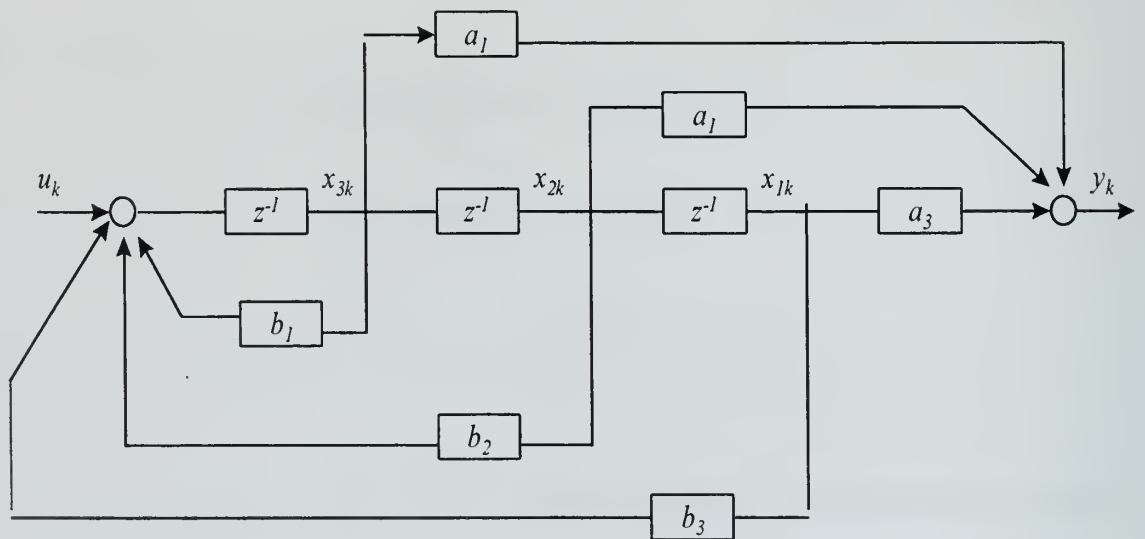

Figure 2.9: State-Space Realization

By inspection

$$x_1(k+1) = x_2(k)$$
$$x_2(k+1) = x_3(k)$$
$$x_3(k+1) = -b_1 \cdot x_3(k) - b_2 \cdot x_2(k) - b_3 \cdot x_1(k) + u$$

$$y = a_1 \cdot x_3(k) + a_2 \cdot x_2(k) + a_3 \cdot x_1(k)$$

In vector-matrix form

$$x(k+1) = \Phi \cdot x(k) + \Gamma \cdot u(k)$$

$$x = \begin{bmatrix} x_1 \\ x_2 \\ x_3 \end{bmatrix} \qquad \Phi = \begin{bmatrix} 0 & 1 & 0 \\ 0 & 0 & 1 \\ -b_3 & -b_2 & -b_1 \end{bmatrix} \qquad \Gamma = \begin{bmatrix} 0 \\ 0 \\ 1 \end{bmatrix}$$

$$y(k) = C \cdot x(k)$$

$$C = [a_3 \quad a_2 \quad a_1]$$

3.   Input/Output Stability

Suppose $|u_k| \le M \le \infty$, for all $k \ge 0$, then P_d is BIBO stable if in response to any

bounded input u_k, the output y_k is also bounded: $|y_k| < \infty$, for $k \ge 0$.

In general, for zero initial conditions, $[\, x(0)=0 \,]$

$$y_k = \sum_{k=-\infty}^{\infty} h_d(k-i) \cdot u_i$$

For BIBO stability

$$|y_k| = \left| \sum_{k=-\infty}^{\infty} h_d(k-i)M \right| \le \sum_{k=-\infty}^{\infty} |h_d(k-i) \cdot M|$$

$$\le M \cdot \sum_{k=-\infty}^{\infty} |h_d(k-i)| < \infty$$

if

$$\sum_{-\infty}^{\infty} |h_d(k-i)| < \infty \qquad \text{or} \qquad \sum_{k=-\infty}^{\infty} |h(k)| < \infty$$

Therefore, if the unit pulse response is absolutely summable, then the system is BIBO stable.

EXAMPLE 2.6: Determine the stability requirements for example problem 2.1.

Consider the unit pulse response

17

$$y_k = h_d(k) = a^k \qquad ; \qquad k=0,1,2,3\ldots\infty$$

and

$$\sum_{k=0}^{\infty} a^k = \frac{1}{1-|a|}$$

is BIBO stable if $|a| < 1$, and unstable otherwise.

D. SIGNAL ANALYSIS AND DYNAMIC RESPONSE

1. Signal Transforms

The unit pulse:

$$U(z) = \sum_{k=-\infty}^{\infty} u_k \cdot z^{-k} = z^0 = 1 \quad ; \qquad u_k = \begin{cases} 1, k = 0 \\ 0, k \neq 0 \end{cases}$$

The unit step:

$$U(z) = \sum_{k=-\infty}^{\infty} u_k \cdot z^{-k} = \sum_{k=-\infty}^{\infty} z^{-k} = \frac{1}{1-z^{-1}} = \frac{z}{z-1} \qquad ; \qquad u_k = \begin{cases} 1; k \geq 0 \\ 0; k < 0 \end{cases}$$

General sinusoid:

$$u_k = r^k \cdot \cos(k\theta) \cdot 1(k) = r^k \left(\frac{e^{jk\theta} + e^{-jk\theta}}{2} \right) \cdot 1(k)$$

$$Z[r^k \cdot \cos(k\theta) \cdot 1(k)] = \frac{1}{2}\left[\frac{z}{z - re^{j\theta}} + \frac{z}{z - re^{-j\theta}} \right]$$

$$U(z) = \frac{z(z - r \cdot \cos\theta)}{z^2 - 2r(\cos\theta)z + r^2}$$

2. Frequency Response of DTS

Consider a sinusoid at frequency ω_0 applied to a continuous-time system

$$u(t) = A \cdot \cos(\omega_0 \cdot t)$$

The continuous-time response is

$$y(t) = A \cdot \cos(\omega_0 \cdot t + \phi)$$

Where the amplitude and phase are defined as

$$A = |G(j\omega_0)|$$
$$\phi = \angle G(j\omega_0)$$

For discrete-time systems

$$u_k = \cos(\omega_0 kT) \cdot 1(t)$$

The discrete transform

$$U(z) = \frac{z(z - r \cdot \cos\omega_0 T)}{z^2 - 2 \cdot r \cdot \cos(\omega_0 T)z + r^2} = \frac{1}{2} \cdot \left\{ \frac{z}{z - e^{j\omega_0 T}} + \frac{z}{z - e^{-\omega_0 T}} \right\} \qquad \text{where } r = 1; \ \theta = \omega_0 T$$

The discrete response

$$Y(z) = G(z) \cdot U(z)$$

$$= \frac{1}{2} \cdot \left\{ \frac{G(z)z}{z - e^{j\omega_0 T}} + \frac{G(z)z}{z - e^{-j\omega_0 T}} \right\}$$

Expanding $Y(z)$ and letting $z \rightarrow e^{j\omega_0 T}$

$$Y(z) = \frac{1}{2} \cdot \left\{ \frac{G(e^{j\omega_0 T})}{z - e^{j\omega_0 T}} + \frac{G(e^{-j\omega_0 T})z}{z - e^{-j\omega_0 T}} \right\}$$

Let $G(e^{j\omega_0 T}) = A(\omega_0 T) \cdot e^{j\psi(\omega_0 T)}$

$$Y(z) = \frac{1}{2} \cdot \left\{ \frac{e^{j\psi} z}{z - e^{j\omega_0 T}} + \frac{e^{-j\psi} z}{z - e^{-j\omega_0 T}} \right\}$$

The inverse transform

$$Y_{ss}(kT) = A \cdot cs(\omega_0 Tk + \psi)$$

3.   The Discrete Fourier Transform (DFT)

Let the time function be periodic, i.e. $f(kT)=f(kT+NT)$, then DFT of $f(kT)$ can be defined as:

$$F\left(\frac{2 \cdot \pi \cdot n}{NT}\right) = \sum_{k=0}^{N-1} f(kT) \cdot e^{-j2\pi(nkT)/(NT)}$$

where $F(n)$ is a z-transform of the $f(kT)$ over one period evaluated at the discrete frequencies of a Fourier series $z = e^{j\omega T}$, where $\omega = 2\pi n \big/ NT$. Define $F_n = F(2\pi n / NT)$, Then the DFT can be rewritten as

$$F_n = \sum_{k=0}^{N-1} f_k e^{-j2\pi(nk)/N}$$

and the inverse transform is

$$f_k = \frac{1}{N} \sum_{n=0}^{N-1} F_n e^{j2\pi(nk)/N}$$

Now evaluating the frequency response using the DFT can be done as follows:

Let

$$u(kT) = A\sin\left(\frac{2\pi lk}{N}\right) ; \qquad \omega_l = \frac{2\pi l}{N}$$

Then

$$U_n = \sum A \cdot \sin\left(\frac{2\pi lk}{N}\right) e^{-j2\pi nk/N}$$

$$= \frac{A}{2j} \cdot \sum \left\{ e^{j2\pi k(l-n)/N} - e^{-j2\pi k(l+n)/N} \right\}$$

$$= \begin{cases} 0; l \neq n \\ \dfrac{NA}{2j}; l = n \end{cases}$$

and the DFT of the output is

$$y(kT) = B \cdot \sin\left(\frac{2\pi lk}{N} + \psi\right)$$

$$Y_n = \sum_{k=0}^{N-1} B \cdot \sin\left(\frac{2\pi lk}{N} + \psi\right) e^{-j2\pi nk/N}$$

$$= \frac{B}{2j} \cdot \sum_{k=0}^{N-1} \left\{ e^{j\psi} \cdot e^{j2\pi k(l-n)/N} - e^{-j\psi} \cdot e^{-j2\pi k(l+n)/N} \right\}$$

$$= \begin{cases} 0; l \neq n \\ \dfrac{NB}{2j} e^{j\psi}; l = n \end{cases}$$

Therefore the transfer function for $\omega_l = \dfrac{2\pi l}{NT}$ is defined by

$$G\left(e^{j2\pi l/N}\right) = \dfrac{Y_l}{U_l}$$

where $Y_l = FFT(y_k)$ and $U_l = FFT(u_k)$, evaluated at $n=l$.

$$G\left(e^{j2\pi l/N}\right) = \dfrac{Y_l}{U_l} = \dfrac{Be^{j\psi}}{A}$$

E.   SAMPLED-DATA SYSTEMS ANALYSIS

For the purpose of studying the sampled-data systems, each operation involved will be analyzed separately. First consider the ideal sampler shown in Figure 2.11. The technique presented here is to use *impulse modulation* to form the mathematical representation for the process of taking periodic samples from $r(t)$ to produce a sequence $r(kT)$ and to analyze the sampled signal as a continuous signal using the Lapace transform.

Figure 2.10 : Ideal Sampler

The output of the sampler is a train of impulses

$$r^*(t) = \sum_{k=-\infty}^{\infty} r(t) \cdot \delta(t - kT)$$

Recall the following properties of the unit impulse

$$\int_{-\infty}^{\infty} f(t) \cdot \delta(t - a)dt = f(a) \qquad \text{sifting property and}$$

$$\int_{-\infty}^{t} \delta(\tau)d\tau = 1(t)$$

Therefore

21

$$\mathrm{L}\left\{r^*(t)\right\} = \int_{-\infty}^{\infty} r^*(t) \cdot e^{-s\tau} d\tau$$

$$= \int_{-\infty}^{\infty} \sum_{k=-\infty}^{\infty} r(\tau)\delta(\tau - kT) \cdot e^{-s\tau} d\tau$$

$$= \sum_{k=-\infty}^{\infty} \int_{-\infty}^{\infty} r(\tau)\delta(t - kT) \cdot e^{-s\tau} \cdot d\tau$$

$$= \sum r(kT) \cdot e^{-skT} = R^*(s)$$

where we used the sifting property of δ.

Now consider the hold operation, which takes the impulses produced by the sampler and extrapolates the data into a piecewise constant output r_h, as shown in Figure 2.12.
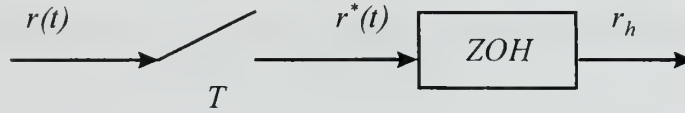

Figure 2.11: Sample and Hold

Using zero-order polynomials, thus, the name zero-order hold (ZOH), which hold each sample constant over the sampling period, the piecewise signal r_h is defined as

$$r_h = r^*(kT) \quad ; \quad kT \leq t \leq (k+1)T$$

The response of the ZOH to a impulse at time $t=0$ is 1 for $0 \leq t \leq T$. The impulse response of the ZOH is $ZOH(t)=1(t)-1(t-T)$. Therefore,

$$ZOH(s) = \int_{0}^{\infty} \left[1(t) - 1(t-T)\right] \cdot e^{-st} \cdot dt = \frac{(1 - e^{-sT})}{s}$$

1.   Spectrum of a Sampled Signal and Aliasing

Since $r^*(t)$ is a periodic function it has a Fourier series representation:

$$\sum_{k=-\infty}^{\infty} \delta(t - kT) = \sum_{n=-\infty}^{\infty} C_n \cdot e^{j(2\pi n/T)t} = \sum_{n=-\infty}^{\infty} C_n \cdot e^{j\frac{2\cdot\pi\cdot n}{T}t}$$

where

$$C_n = \frac{1}{T} \int_{-T/2}^{T/2} \sum_{k=-\infty}^{\infty} \delta(t-kT) \cdot e^{-jn(2\pi/T)t} \, dt$$

$$= \frac{1}{T}$$

Therefore,

$$\sum_{k=-\infty}^{\infty} \delta(t-kT) = \frac{1}{T} \sum_{n=-\infty}^{\infty} e^{j(2\pi n/T)t}$$

Let $\omega_s = \dfrac{2\pi}{T}$, be the sampling frequency and take the Laplace transform of the sampler output:

$$L(r^*(t)) = \int_{-\infty}^{\infty} \left(\sum_{n=-\infty}^{\infty} r(t) \cdot \delta(t-kT) \right) e^{-st} \, dt$$

$$= \int_{-\infty}^{\infty} r(t) \left\{ \frac{1}{T} \sum_{n=-\infty}^{\infty} e^{jn\omega_s t} \right\} e^{-st} \, dt$$

$$= \frac{1}{T} \sum_{n=-\infty}^{\infty} \int_{-\infty}^{\infty} r(t) \cdot e^{jn\omega_s t} \cdot e^{-st} \, dt$$

$$= \frac{1}{T} \sum_{n=-\infty}^{\infty} R(s - jn\omega_s)$$

Let $s = j\omega$

$$R^*(j\omega) = \frac{1}{T} \sum_{n=-\infty}^{\infty} R(j\omega - jn\omega_s)$$

Notice, that sampling produces an infinite train of sidebands at $n\omega_s, n = -\infty \ldots \infty$.

EXAMPLE 2.7: Let $\omega_s = 1$, $\omega_l = 1/8$

$$R^*(j1/8) = \ldots + R(j\omega_1) + R[j(\omega_1 - \omega_s)] + R[j(\omega_{21} - \omega_s)] + \ldots$$

$$= \ldots + R(j1/8) + R[j(-7/8)] + R[j(-14/8)] + \ldots$$

If $R(j\omega)$ has components above the Nyquist frequency $\omega_s/2$ or π/T, then after sampling overlap or aliasing will occur and the original signal can not be reconstructed. This leads

23

to the sampling theorem: the original signal can be recovered from its samples if the sampling frequency ($\omega_s = 2\pi/T$) is at least twice the highest frequency in the signal. To avoid aliasing a low-pass anti-alias filter is usually inserted preceding the sampling operation.

2.   Data Extrapolation

To recover $R(j\omega)$ pass R^* through a low-pass filter $L(j\omega)$ as shown in Figure 2.12.
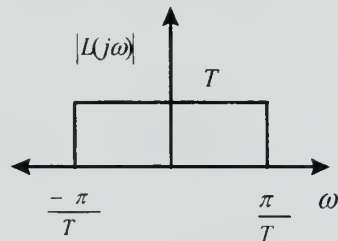
$$R(j\omega) = L(j\omega)\, R^*(j\omega)$$

Figure 2.12: Ideal Lowpass Filter

Then

$$l(t) = \frac{1}{2\pi} \int_{-\pi/T}^{\pi/T} T \cdot e^{j\omega t}\, d\omega$$

$$= \frac{T}{2\pi j t}(e^{j(\pi/T)} - e^{-j(\pi/T)})$$

$$= \frac{1}{\pi t/T}\sin\frac{\pi t}{T}$$

$$= \mathrm{sinc}\frac{\pi t}{T}$$

Therefore,

$$r(t) = \int_{-\infty}^{\infty} r^*(\tau)\cdot l(t-\tau)\cdot d\tau$$

24

$$= \int_{-\infty}^{\infty} \sum_{k=-\infty}^{\infty} r(\tau) \cdot \delta(\tau - kT) \cdot \text{sinc} \frac{\pi(t-\tau)}{T} d\tau$$

$$= \sum_{k=-\infty}^{\infty} r(kT) \text{sinc} \frac{\pi(t-kT)}{T}$$

Note, the ideal extrapolator is noncausal, since $l(t)$ is nonzero for $t < 0$. Suppose $L(jw)$ is replaced by ZOH.

Recall,

$$ZOH(j\omega) = \frac{1 - e^{-j\omega T}}{j\omega}.$$

Expressing the transfer function in magnitude and phase form

$$ZOH(j\omega) = T \cdot e^{-j\omega T/2} \text{sinc} \left(\frac{\omega T}{2} \right)$$

Therefore,

$$|ZOH(j\omega)| = T \left| \text{sinc} \frac{\omega T}{2} \right|$$

$$\angle ZOH(j\omega) = \frac{-\omega T}{2} + 180 \cdot \delta(\omega - n2\pi)$$

The resulting signal contains unwanted harmonics or impostors. By frequency analysis of $r(t)$ the principal harmonic can be identified.

Consider the sinusoid signal $v(t) = e^{j\omega_0 t + j\phi}$

$$V(j\omega) = \int_{-\infty}^{\infty} e^{(j\omega_0 t + j\omega\phi)} \cdot e^{-j\omega t} dt$$

This integral is not defined, however notice $Z(\delta(t)) = \int_{-\infty}^{\infty} e^{-j\omega t} \cdot \delta(t) \cdot dt = 1$,

$$\delta(t) = \frac{1}{2\pi} \int_{-\infty}^{\infty} e^{j\omega t} d\omega.$$

Now replace t with ω to get

$$\delta(\omega) = \frac{1}{2\pi} \int_{-\infty}^{\infty} e^{j\omega t} dt$$

Therefore,

$$V(j\omega) = \int_{-\infty}^{\infty} e^{\left(j\omega_0 t + j\phi\right)} \cdot e^{-j\omega t} dt$$

$$= 2\pi e^{j\phi} \delta(\omega - \omega_0)$$

Since δ is a even function, the spectrum of $r(t)$ can be written in terms of impulse functions

$$R(j\omega) = \pi A \left[e^{j\phi} \delta(\omega - \omega_0) + e^{-j\phi} \delta(\omega + \omega_0) \right]$$

To recover the signal R_h, multiply the spectrum of R^* by the transfer function of the ZOH.

F. DISCRETE EQUIVALENTS BY NUMERICAL INTEGRATION

Concept: Represent a given continuous transfer function $H(s)$ as a differential equation and derive a difference equation whose solution is an approximation to that of the differential equation.

1. Numerical Integration

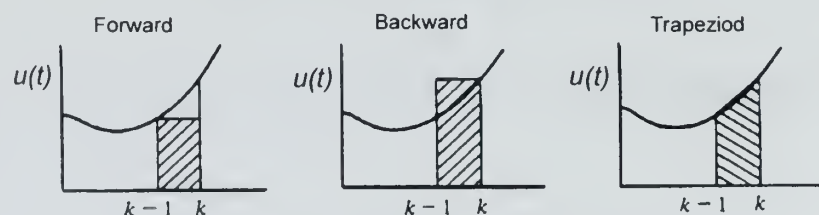When considering discrete approximation to integration, as shown in Figure 2.13, three alternatives exist.

Figure 2.13: Area Approximation Rules

Approximation methods:

Forward:

$$Z\{x_{k+1} = x_k + T \cdot (u_k)\}$$

$$\left.\begin{array}{l} zX(z) = X(z) + T \cdot U(z) \\ X(z)(z-1) = T \cdot U(z) \end{array}\right\} \Rightarrow H(z) = \frac{X(z)}{U(z)} = \frac{T}{z-1}$$

s is replaced by $\rightarrow \dfrac{z-1}{T}$

Backward:

$$Z\{x_k = x_{k-1} + T \cdot u_k\}$$

$$X(z) = z^{-1}X(z) + T \cdot U(z) \Rightarrow H(z) = \frac{X(z)}{U(z)} = \frac{T}{(1-z^{-1})}$$

s is replaced by $\rightarrow \dfrac{z-1}{Tz}$

Trapezoid Rule (Tustin's Method):

$$Z\{x_k = x_{k-1} + \frac{T}{2} \cdot (u_k - u_{k-1})\}$$

$$(1-z^{-1}) \cdot X(z) = \frac{T}{2}(1-z^{-1}) \cdot U(z) \Rightarrow H(z) = \frac{X(z)}{U(z)} = \frac{T}{2} \cdot \frac{1+z^{-1}}{1-z^{-1}} = \frac{T}{2} \cdot \frac{z+1}{z-1}$$

s is replaced by $\rightarrow \dfrac{2}{T}\dfrac{z-1}{z+1}$

Therefore, given a continuous transfer function H(s) a discrete equivalent can be found by the substitution:

$$H_t(z) = H(s)\big|_{s=(2/T)[(z-1)/(z+1)]}$$

27

2.   Zero-Pole Mapping Equivalents

This technique consists of a set of rules for locating the zeros and poles and setting the gain of a *z*-transform that will describe a discrete, equivalent transfer function that approximates the given *H(s)*.

Rule #1: All poles of *H(s)* are mapped by $z = e^{sT}$. Replace *s* with e^{sT} for the poles of *H(s)*. If *H(s)* has a pole at $s = a$, then *H(z)* has a pole at $z = e^{-aT}$. If *H(s)* has a complex pole at $s = -a + jb$, then *H(z)* has a pole at $z = re^{\pm j\theta}$.

Rule #2: All finite zeros are mapped by $z = e^{sT}$.

Rule #3: All infinite zeros of *H(s)* are mapped by $z = -1$.

a)   Only one zero of *H(s)* at $s = \infty$ is mapped into $z = \infty$.

Rule #4: The gain of the digital filter is selected to match the gain of H(s) at the band center.

$$H(s = 0) \Rightarrow H_d(z = 1)$$

3.   Zero-Order Hold Equivalent

If the approximating hold is the ZOH, then the equivalent to *H(s)* is

$$H(z) = (1 - z^{-1})Z\left\{\frac{H(s)}{s}\right\}$$

This is the same relationship that was derived earlier in section C of this chapter.

III. INTRODUCTION TO RAPID PROTOTYPING

The primary tool for the research conducted in the Avionics lab is the hardware/software interface provided by the MATRIX$_x$ product family developed by Integrated Systems Inc. (ISI). The MATRIX$_x$ product family is shown in Figure 3.1. This software provides a complete workbench for control systems design and implementation. The RealSim controller automates the development of the real-time systems by combining graphical modeling software with real-time control hardware. The key feature of this product is the AutoCode tool which will automatically program higher-language code such as C or ADA for the designed controller. The software consists of an easy to use graphical user interface (GUI) that can be run on either SUN workstations or a PC. The interface interacts with a high-speed digital signal processing (DSP) board developed by Texas Instruments. The system is called AC-100 Model C30.
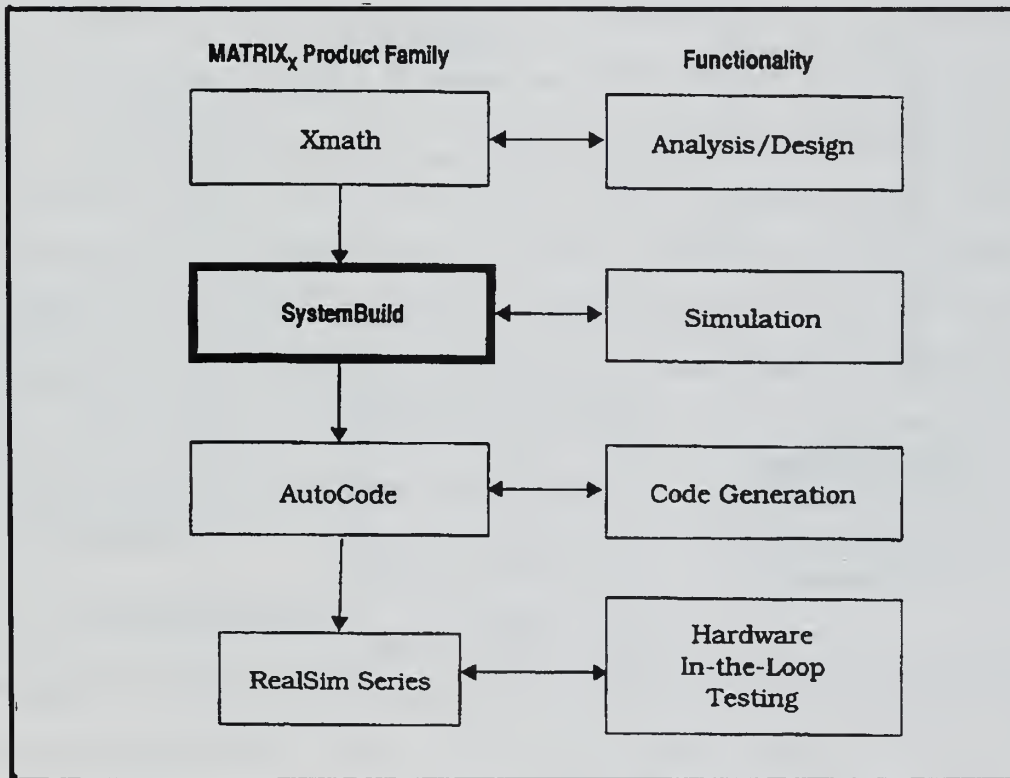

Figure 3.1: MATRIX$_x$ Product Family

29

A. RAPID PROTOTYPING SYSTEM ARCHITECTURE

The rapid prototyping system architecture consists of a UNIX workstation and a windows based PC host computer which is equipped with two ISA bus adapter boards (Figure 3.2). The workstation and PC are connected through Ethernet, using the standard TCP/IP protocol suite. The two hardware boards in the PC consist of a board which acts as the motherboard for the C30 DSP, and a "DSPFLEX" carrier board which holds four input/output, or "IP", modules. The I/O boards connect the model to the real hardware via the Hardware Connection Editor (HCE), which will be discussed in later sections. The complete system is referred to as the AC-100 Model C30 real-time controller.

The avionics lab currently has two PC's configured as described above: a Pentium tower PC called *America* and a luggable PC called *AC100*. The luggable PC is normally
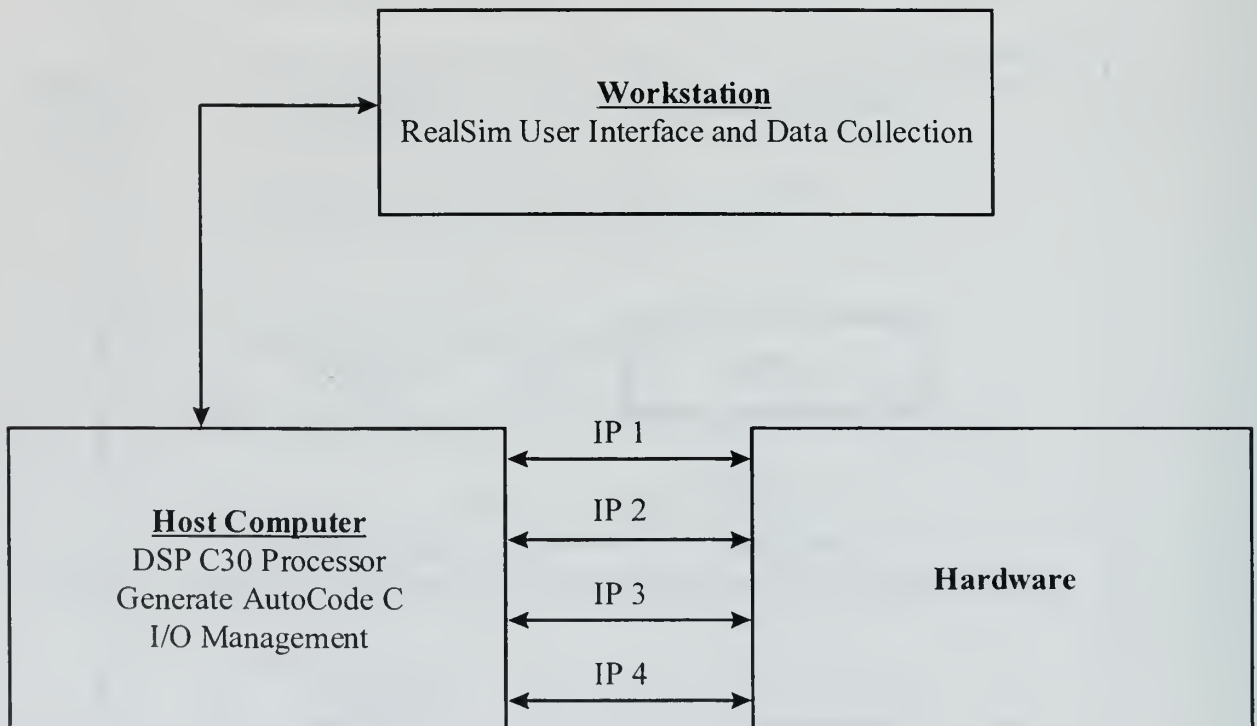

Figure 3. 2 : RealSim Architecture

connected to a stand alone Sparc II workstation, used for field fight testing with the school's Unmanned Air Vehicle (UAV) called *FROG*.

There are a number of different types of I/O cards available depending on the application. Currently both PC's have 4 IP modules consisting of a serial communication (IP_Serial) module, digital-to-analog (IP_DAC) module, analog-to-digital (IP_HiADC) module, and a pulse width modulation (IP_68332) module. A description of each IP module and procedures for connecting hardware to the model is covered in detail in the Hardware-In-The-Loop Testing section of this thesis.

B. XMATH/SYSTEMBUILD

Xmath/SystemBuild is a software program similar to the Matlab/Simulink software programs. Xmath is the parent process and will launch the SystemBuild editor when the build command is given or when a file is loaded that contains SystemBuild data. It was designed to include an extensive set of design and analysis functions for both the classical input/output control techniques and the modern state-space control techniques. The SystemBuild program uses a hierarchical method of organization, based on the SuperBlock concept. SuperBlocks provide a way of organizing a group of blocks that define a function into a compact form for display. Through the use of this hierarchy, variable names can be passed up and down the hierarchical structure allowing the engineer to easily track and understand what variables are and where they interact with the model. This section will cover the basic functions of Xmath/SystemBuild, for detailed information refer to [Ref. 4].

1. Xmath Basics

Xmath can be run from either the SUN or SGI workstations located in the avionics and aeronautics labs. Prior to using the MATRIX$_x$ software, the user must configure his UNIX account to source the 'ac100setup' file which defines the editor used by the system. This command should be set up as a marcro in the user's .cshrc file so it

31

will automatically run each time the user logs on to the workstation. Adding the following command line to the .cshrc file: 'source$ISI/AC100/bin/ac100setup.sh`, will accomplish this.

Before invoking Xmath, a separate directory for each project should be created to avoid using project files from one project with the standard files of another project. Therefore, start by first creating a project directory and then move to that new directory using the following UNIX commands: **mkdir *project_name*, cd *project_name*.** To start Xmath type << *xmath* >> in the console window. This will bring up the Xmath command window as shown in Figure 3.3.
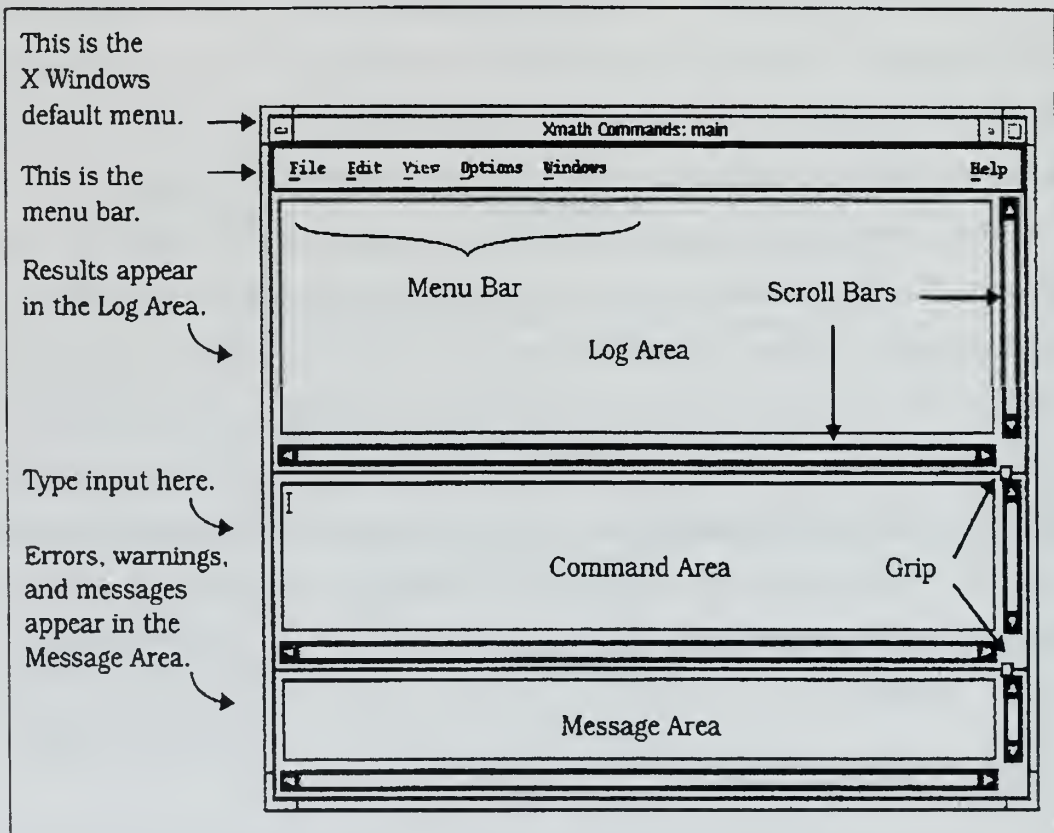

Figure 3.3: Xmath Command Window

2.   SystemBuild Modeling

This section is a tutorial that covers the basics of the SystemBuild editor and simulator. In the following example, the user will build a block diagram and simulate its operation. The model for this illustration is a simple Speed_Controller shown below in Figure 3.4.
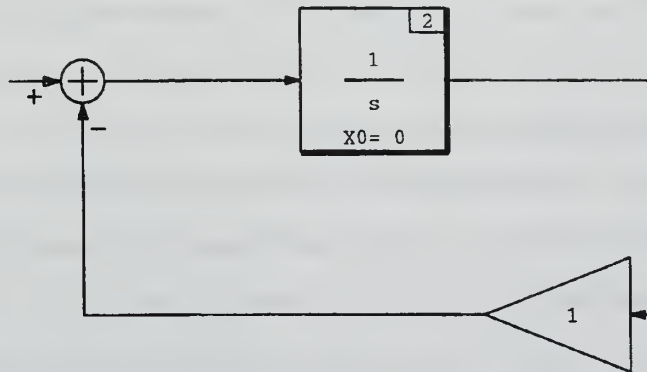
Figure 3.4: Speed_Controller

Step 1: Defining the SuperBlock

To invoke SystemBuild, at the Xmath command line type << *build* >> and press return. The SystemBuild menu bar will appear across the top of the display. Select **Build** from the menu bar with the left mouse button. Then select **Edit SuperBlock** from the Build menu. The Edit SuperBlock dialog box will appear and initially the menu in the box is empty. Click the left mouse button on **Edit New SuperBlock**, and the SuperBlock Attributes dialog box appears. Using the SuperBlock Name field, name the SuperBlock. Under Type, select **Continuous** and click **DONE**.

Step 2: Placing the Blocks

A new SystemBuild editor window should be displayed, ready for building the block diagram. To select from the SystemBuild block library, click on **Define Block** from the Edit menu or, using a shortcut, double-click in the empty window to bring up the SystemBuild block menu. The SystemBuild blocks are grouped together in thirteen

palettes. To select a palette, click on one of the three-letter combinations at the top of the menu.

To begin building the Speed_Controller, first select the **Gain** Block from the algebraic block palette (ALG). Click and hold the left mouse button on this block, drag it into the screen, and release the mouse button when the Gain block dialog box appears, name the block, if desired, and click **DONE**. Next, select the **Summer** block from the AGL palette and the **Inegrator** block from the DYN palette using the same procedures.

Step 3: Connecting the Blocks

The next step is to connect the blocks. Note the middle mouse button will be used to make connections. Start by connecting the Summer block with the Integrator block. Click in the Summer block, with the middle mouse button, then click on the Integrator block. A line should connect the two blocks. Using the same procedure, connect the Integrator to the Gain block. Now, connect the Gain block to the Summer block. Since there is more than one input to the Summer, the Connection Editor will appear as shown in Figure 3.5. Use the connection editor to specify the connections; the inputs to a block
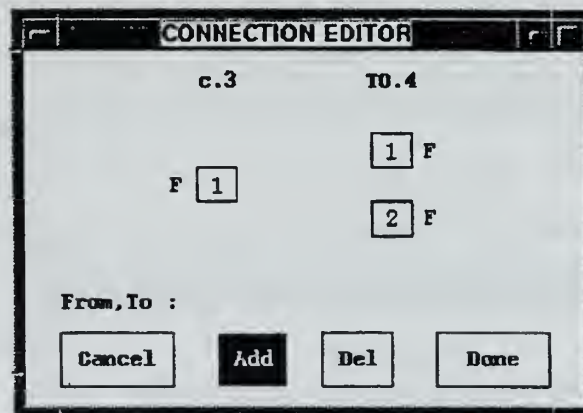

Figure 3.5: Connection Editor

are in numerical order from top to bottom. The output from the Gain block should go to the second input of the Summer. Then with the left mouse button' connect to Gain block with the number 2 Summer input, highlight **Add** and click **Done.**

Note that the blocks can be resized by clicking on the block id number and moving the mouse, or flipped by double-clicking on the block's body.

Step 4: Connecting External Inputs and Outputs

Input connections: click the middle mouse button in the open space, then in the Summer block. The connection editor dialog box appears. With the left mouse button, click the number 1 port of the Summer block then click Done. To label the external input, click and hold the left mouse button in the SuperBlock ID bar, just above the SystemBuild window. Select SuperBlock Attributes. In the dialog box, select the **Labels** tab and under **Input Naming** select **Enter Local Label Names.** Now select the **Input** tab and beside **Input Label** type the desired name. Click **Done.**

Output connections: With the middle mouse button click in the integrator block, then click in an open space. Connect the two boxes, then click **Done.**

Simulating the Model

The Speed_Control model can now be simulated. There are a number of different methods to simulate model, two of which are described here;

Method 1: First define a time-vector in Xmath by specifing a name, range, and an increment. In the Xmath command window type: $<< t=[0 : .1 : 20]' >>$;. Next, specify an input vector of magnitude one: $<< u=ones(t) >>$;. Enter the simulation command. Type: $<< y=sim("Name of SuperBlock", t , u) >>$;. Note in this example the name of the SuperBlock is *Speed_Controller*. This command invokes the simulator, specifies that the Speed_Controller model SuperBlock is to be processed, and sets the output equal to y. After the simulation is complete, plot the output by typing: $<< plot(y) >>$. Note, more details on using the sim command are available by typing $<< help sim >>$ in the Xmath command window.

Method 2: From the menu bar under analysis select **Simulation.** This will bring up the simulation parameter dialog box. Define a time vector and input vector as above and run.

Analyzing the Model

The Xmath/SystemBuild software contains an extensive set of functions for system analysis. Specifics for analyzing the model can be found in the Xmath and SystemBuild Core Manuals located in the avionics lab or by using the help command.

To linearize the model, the Xmath command is $<<$ *sys=lin("SuperBlock name",{keywords})* $>>$, where *sys* is the name of the Xmath system object in state-space form. Other useful commands include*: poles(sys), eig(a),bode(sys).*

Saving the Model

To save the model select **File** from the menu bar, highlight the SuperBlock name and click on **Save**.

C.   REALSIM SERIES RAPID PROTOTYPING

This section will continue with the design of the speed controller presented in the last section. The tutorial will demonstrate the basic procedures for using the GUI and testing on a real-time controller. Later sections will describe how the hardware is connected to the model and the procedures for hardware-in-the-loop testing.

1.   RealSim Graphical User Interface (GUI)

Each RealSim project is placed in a unique RealSim project directory. A number of standard files are associated with each RealSim project. Therefore it is recommended to create a separate project directory for each project. The project name and the directory name should be the same.

To invoke the RealSim GUI type $<<$ *realsim* $>>$ in the UNIX command window. When the RealSim GUI is invoked in a new directory a dialog box will appear along with the GUI. Pressing return or clicking yes in the dialog box will enable the makeproject command which creates the first of the required standard files called animation configuration file (animation.cfg). Once all the default settings have been accepted, the project name in the bottom left-hand corner of the GUI should be listed.

Next the user must create a target configuration file (target_config.cfg) file. This file contains information such as the settings that the AutoCode needs to generate the appropriate C code, which controller the model is to run, how many processors are in the controller. This file will be used later to compile, link, download and run the design. To create this file, click on show utilities in the GUI and select **Retarget**. The target is the node name of the controller. In the UNIX command window the user will be asked for the 'controller host name[ ]:' which in the avionics lab is '*america*.' All of the remaining default settings should be accepted. After retargeting the system to '*america*' the GUI should indicate this in the middle of the bottom line in the GUI, see Figure 3.6.

These files are only created once for each project, as long as there are no changes to the system configuration. Once these standard files have been set up for a specific project, and the user is in the project directory for that project, typing $<<$ *realsim* $>>$ in the UNIX command window will start the GUI targeted accordingly.

Through the use of the GUI the designer can now follow the flow diagram that steps the user through the design process. As the user performs each step of the process, the GUI paths are filled in, indicating the current stage in the design process. If certain RealSim files are older than their logical predecessors, the Needs Up dating indicator will be displayed.

2.   Building the Model

The first step in the process is building the model using Xmath/SystemBuild, as described in the previous section. To continue with the **speed controller** model, click on the **Xmath/SystemBuild** block in the GUI. This will bring up the Xmath command

37

window. From this window, select **file** and **load** from the menu bar. Highlight the file name and click **OK**. Select the SuperBlock from the build menu to display the model of the Speed_Controller.
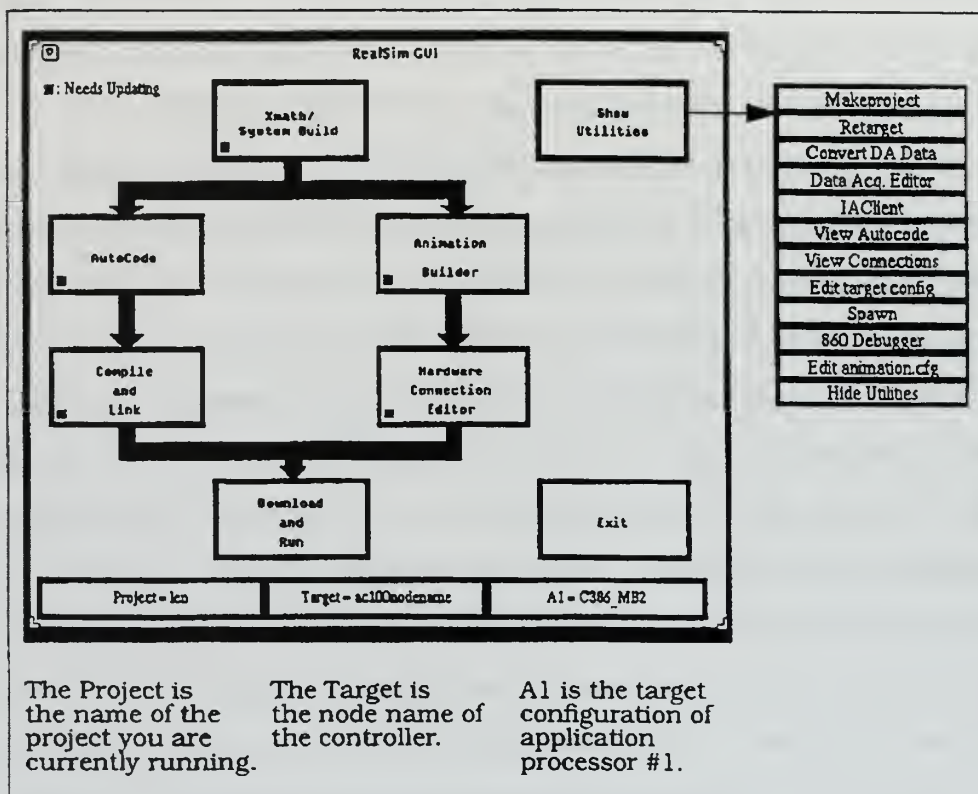

Figure 3.6: RealSim Graphical User Interface

The SuperBlock design, for this example, is presently a continuous type and needs to be transformed to a discrete controller (z-domain). Selecting **Transform SuperBlock** under **Build** from the menu bar will display the transform dialog box. Highlight the SuperBlock name and under type select **Discrete**, then click **Transform**. When transforming from continuous-time to discrete-time a time delay block must be added to the block diagram, as shown in Figure 3.7. From the DYN palette select the time delay block.
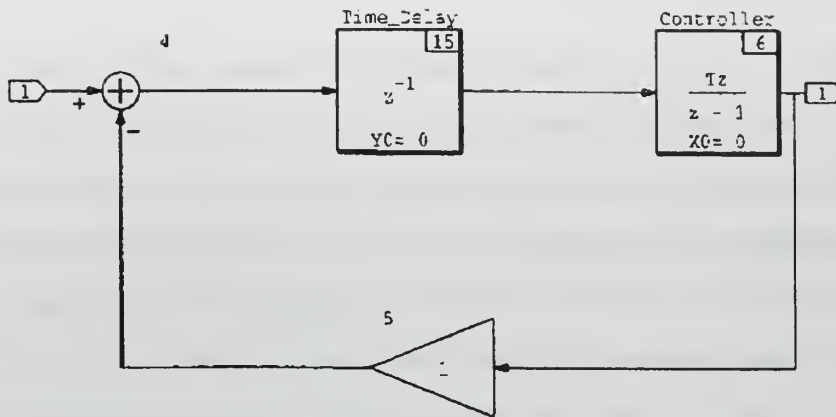
38

Figure 3.7 : Discrete SuperBlock for Speed Controller

3. AutoCode

Once the SuperBlock is complete, the user must generate real-time code. In SystemBuild, select **Generate Real-Time Code** from the Build pull-down menu. When the dialog box appears, highlight the SuperBlock for which you want to generate code. Beside the generated code language, select **RTF_only**, and check that the filename is the same as the project name, then click **DONE.** This produces a file with the model name followed by a .rtf extension. This file containing the real-time code is a top level input/output code that is used by the AutoCode program to produce a higher-level language used to conduct hardware-in-the-loop testing.

After the user has generated a real-time file from the SystemBuild model, invoke the AutoCode by clicking the **AutoCode** button in the RealSim GUI. The AutoCode high-level language code generator reads the real-time (or .rtf) file and produces a high-level source code file with the extension of .c. This file will be used to compile, link, and run the design. The GUI should now indicate the completion of the AutoCode process.

39

4. Interactive Animation

The next step is to build the Interactive Animation (IA) picture display for monitoring and controlling the model while it is being executed in the workstation simulation environment or during hardware-in-the-loop testing. Invoke the editor by clicking on the Interactive Animation Builder button in the GUI. The animation diagram is made by selecting icons from a given library of gauges, dials, switches, and other various input and output devices. The Interactive Animation section of the AC100 User's Guide [Ref. 4] has details on all of the available icons. Selecting **DEFINE** from the IA control panel will display the library of icons. For the Speed_Controller example select the dial for the input and a digital readout for the output as shown in Figure 3.8. The **RTF NAMES** button in the control panel loads the I/O names from the model .rtf file and must be loaded prior to making any connections. Using the IA Connection editor, similar to the SystemBuild editor, the appropriate inputs and outputs are connected to the appropriate devices. Once the picture is complete select **SAVE PICT** from the control panel and a file with a .pic extension is created in the working directory.
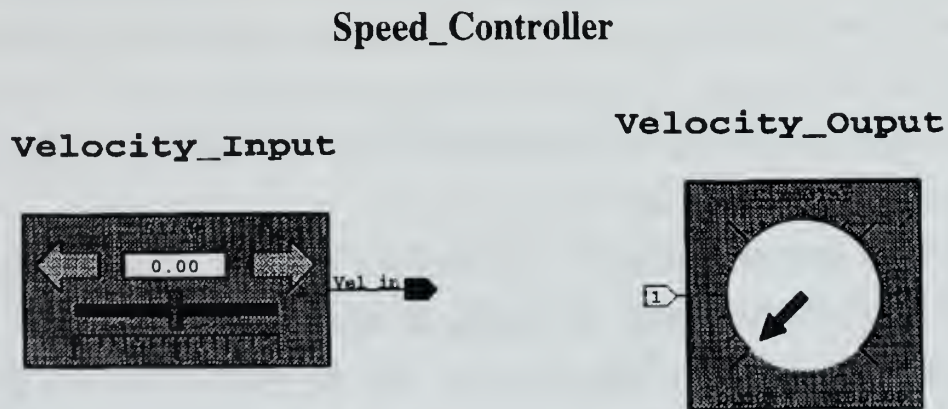
Speed_Controller

Figure 3.8: IA Speed_Controller

5.   Hardware Connection Editor (HCE)

The Hardware Connection Editor is used to make connections from the external I/O in the SystemBuild model to either external hardware I/O devices for hardware-in-the-loop testing or to the IA module for simulation. Before invoking the HCE, the user should have a copy of the file 'c_c30.hce' in the project directory. This file informs the HCE what type of external I/O devices the target computer, *America*, is equipped with. This process will be covered in greater detail, along with the current set-up in the avionics lab, in the Hardware-In-The-Loop Testing section of this thesis.

Two connection editors will appear when starting the HCE. The first screen is for the SuperBlock external inputs and the second for external outputs (see Figure 3.9).   For this example, the input device will be '**MONITOR_INPUT**' type. No changes should be required to the editors and the only action by the user should be to click **DONE** to both pages.
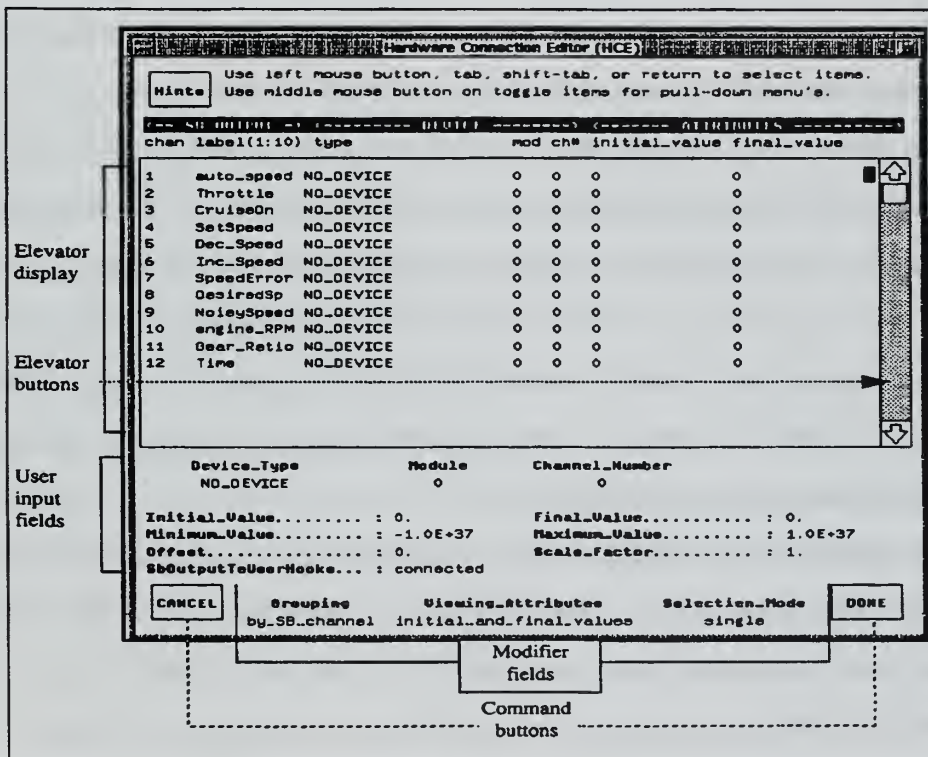

Figure 3.9: HCE

6. Compile and Link

Once the AutoCode is complete the C source files need to be compiled and linked to the C30. Selecting the **Compile and Link** button in the RealSim GUI will cause the UNIX systems to connect via ftp with the AC100 target computer (*America*). For this to happen the host computer, *America,* must be in the ftp mode. Typing 'ac100svr' at the DOS prompt on *America* will enable the computer for ftp transfer. The compiler generates object code from the .c file and the link creates a C30 DSP executable from the object code.

7. Download and Run

When all the above steps are completed, the model is ready to be tested. The testing for this illustration will be a simulation only, since no hardware is connected. Selecting Download and Run on the GUI will connect the RealSim software to the target AC100 computer through ftp. Once the connection is made, it will automatically load the C30 executable into the C30 memory and prepare it to run. The IA module will appear on the workstation window along with a control panel called IA Client, see Figure 3.10.

The START CONTROLLER button starts the execution of the model using the initial values loaded from the *project_name.ioc* file for the external inputs, and outputs defined by the SystemBuild model. The STOP CONTROLLER button stops the executing application and holds the external inputs and outputs at their final values. The RESTART CONTOLLER button restarts the model, again using the initial values that were loaded from the *project_name.ioc* file.

The HARDWARE RESET button causes the RealSim controller to perform a hardware reset and causes the IA Client to exit. This is the best way to exit after a run, as it will clear the C30 memory and return the AC100 computer to a ready status. The third button, EXIT GRAPHICS, exits the IA Client without rebooting the controller. This is a software reboot only, which stops the model and terminates the ftp connection. This button is not recommended for use, as it will not stop the model from running on C30.
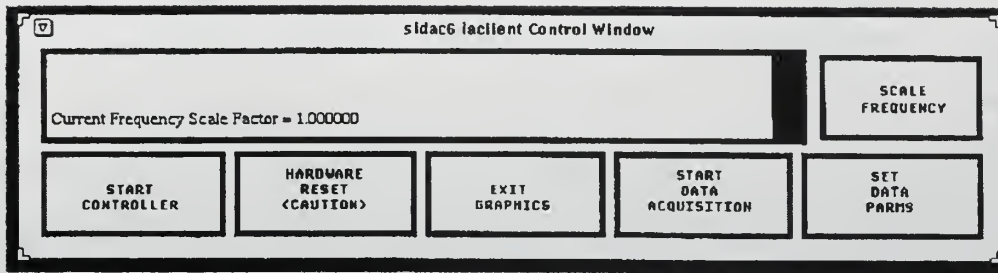
Figure 3.10: IA Client

8. Data Acquisition Editor

The RealSim data acquisition editor defines one or more data acquisition sets for each project and provides real-time data acquisition. This allows the user to record and analyze any of the inputs or outputs associated with the project. To invoke the data acquisition editor select 'Data Acq. Editor' from the show utilities button in the GUI. The first data acquisition screen to appear contains all the inputs to the system. The user selects the desire inputs for recording by highlighting the variable and selecting 'ON' next to the **DA_Setting** modifier field at the bottom left of the screen. The **'DA_Decimation_Factor'** should read '1', this ensures the value will be recorded every time step. To select the outputs for recording, toggle the '**Display**' selector at the bottom of the screen from the 'SB_INPUTS' to 'SB_OUTPUTS'.

The START DATA ACQUISITION button starts/stops the data acquisition program which will record any or all of the inputs and outputs to the C30. Starting the data acquisition creates a file in the project directory with the project name and '_1.raw' extension. Each time the acquisition process is started a new file is created and the number will increment up corresponding to the number of data files created. Therefore it is good practice to note which data files correspond to which runs when testing.

To retrieve the data after the exiting the controller, the user selects 'Convert DA Data' from the show utilities button in the GUI. The workstation command window will show the last data file recorded with a '.dat' file extension. The user can accept the file listed in the window by pressing return or select a previous file by changing the number

of the file. This process creates a file with the same name as the corresponding raw file that can now be loaded directly into Xmath for analysis. The variable names will be the same as those used as the input or output names in the SystemBuild model. These variables will be vectors with lengths depending on the amount of time that data was recorded. A reference file is also created when converting the data that contains specific information on that data file, such as the amount of time recorded or the number of elements in the file. This will help identify data files if numerous runs are made during testing.

IV. HARDWARE-IN-THE-LOOP (HITL)

This section outlines the process of connecting hardware to a digital controller. By using the standard input/output devices integrated with the RealSim software, the SystemBuild diagram is connected to the desired hardware. A critical part of connecting hardware to the controller is the calibration of the sensors. The controller uses an algebraic conversion of the measured sensor output signal from the hardware. This algebraic conversion requires calibration by determining the correct conversion constants.

To demonstrate this step of the design process in the avionics lab, a device called the Airborne Remotely Operated Device, AROD, will be used. The lab currently has two AROD devices which the students will use for calibration and HITL testing. A complete description of the AROD is given in [Ref. 5].

A. HARDWARE DESCRIPTION FOR AROD

The control surfaces of the AROD are actuated by Futaba FP S34 servo motors. To control these actuators, a Pulse Width Modulation (PWM) input signal is used. The width of the pulse determines how far the servo will turn. The internal control circuit of the Futaba motor includes a small potentiometer in a feedback loop to sense the servo position. The output signal from this sensor is noisy due to the varying current draw during motor operation. Therefore, the actuators installed on the AROD in the lab have been modified to reduce sensor noise. An additional wire has been added so that the positive voltage on the potentiometer could be measured at the same time as the center voltage [Ref. 5]. Taking the difference between the measured high voltage V_H and the centered voltage V_C, give a delta voltage V_D and results in a significant reduction in sensor noise. This set up is shown in Figure 4.1.
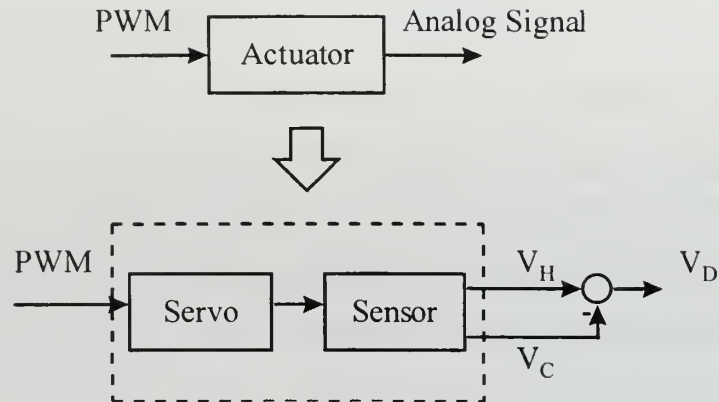
Figure 4.1: Futaba Actuator

B.   CONVERSION SUPERBLOCKS

For this design, the controller input commands are given in degrees. Since the input signal to the actuators operates on PWM, a conversion from degrees to PWM must first be implemented. Similarly, the output signal from the sensors must be converted from volts to degrees. Figure 4.2 shows the SuperBlocks that will be developed to implement this design.
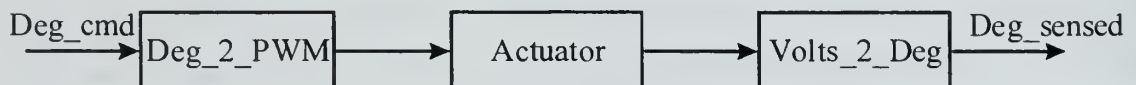

Figure 4.2: Conversion SuperBlocks

1.   Converting Degrees to PWM

Previous testing of the actuators has determined the total throw to be 0 to 200 degrees, with a pulse width of 0.6 milli-seconds corresponding to the minimum deflection, 2.4 milli-seconds corresponding to the maximum deflection, and a pulse-width of 1.5 milli-seconds corresponds to the centered position, [Ref. 5].

46

The refresh frequency for the AROD HITL test was chosen to equal the controller frequency of 25 Hertz, giving a period T of 40 milli-seconds. Figure 4.3 depicts the relevant quantities for a PWM signal.
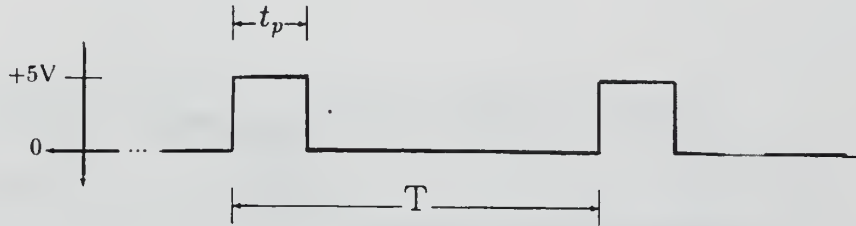

Figure 4.3: PWM

Duty cycle is calculated as:

$$Duty\ Cycle = \frac{t_p}{T}$$

A minimum pulse width of 0.6 milli-seconds, corresponding to −100 degrees, results in a duty cycle of:

$$Min.\ Duty\ Cycle\ (\text{-}100\ deg.) = \frac{0.6}{40} = 0.015$$

The maximum pulse width of 2.4 milli-seconds, corresponding to +100 degrees, results in a duty cycle of:

$$Max.\ Duty\ Cycle\ (\text{+}100\ deg.) = \frac{2.4}{40} = 0.06$$

Assuming a linear relationship from minimum to maximum values, the following function is used to determine the required duty cycle for a given input in degrees.

$$Duty\ Cycle\ = 0.0002 * (Desired\ deflection\ in\ degrees) + 0.0375 \qquad \text{(Eq. 4.1)}$$

The algebraic block '*Deg_2_PWM*' shown in Figure 4.4 implements this equation.
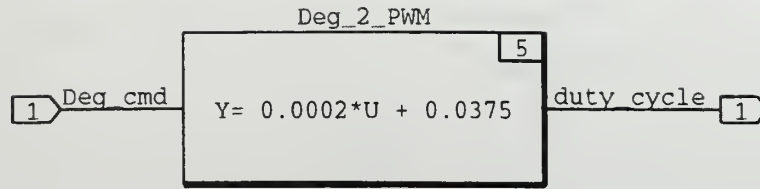
Figure 4.4: Deg_2_PWM SuperBlock

2. Converting Volts to Degrees

The output signal from sensors on the AROD, as described above, is the difference between the measured high voltage V_H and the centered voltage V_C. This voltage signal must be converted to the correct vane position in degrees for feedback to the RealSim controller and user display. Again it is assumed that there is a linear relationship from minimum to maximum deflection as shown in Figure 4.5.
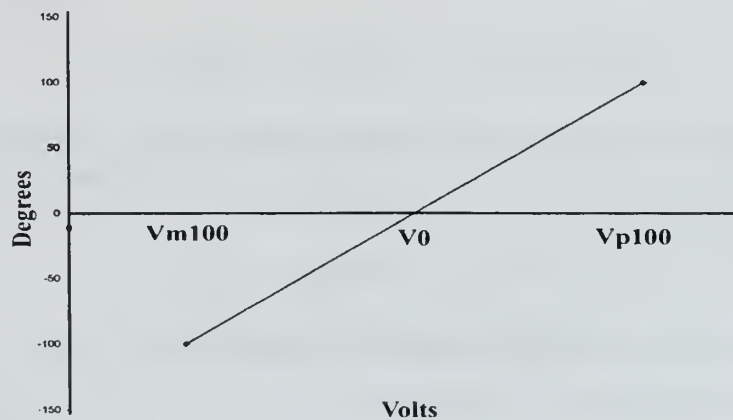

Figure 4.5: Volts to Degrees Conversion

Therefore the measured output voltage from the sensor can be converted into correct vane position in degrees by:

$$Deg\_out = \frac{200}{V_{p100} - V_{m100}} \cdot (V_D - V_0)$$ (Eq. 4.2)

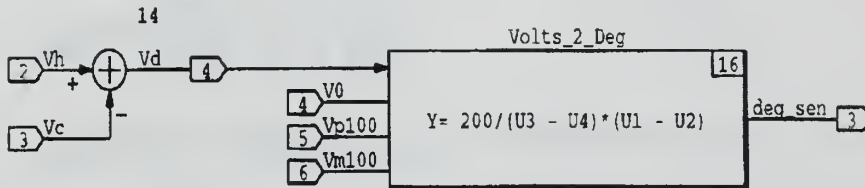The algebraic block '*Volts_2_Deg*' shown in Figure 4.6 implements this equation.

Figure 4.6: Volts_2_Deg SuperBlock

C.   SENSOR CALIBRATION

Before the sensors can be used reliably by the controller, they must be calibrated. Due to small changes in the operating voltages, calibration is required each time the controller is started.   The calibration process illustrated here for the AROD involves measuring the sensed voltages for vane positions of maximum deflection (–100 deg), minimum deflection (+100 deg), and the centered position (0 deg.).   These measured voltage values are then used in Equation 4.2 to obtain the correct vane position. Referring to the Calibration IA screen shown in Figure 4.7, the calibration procedures are:

- Command zero degrees of deflection using the 'Deg_cmd' dial.   Input the displayed voltage into the window labeled 'V0'.

- Repeat step 1 for max. (+100 deg.) deflection and min. (-100) deflection.

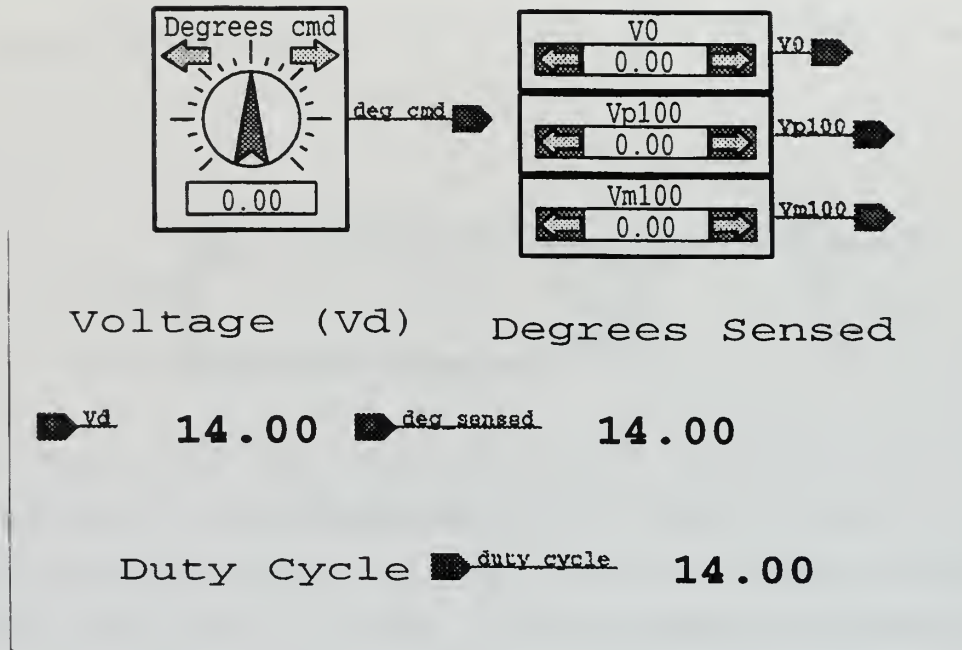- Confirm that the degrees sensed are the same as the commanded degrees.

Calibration

Figure 4.7: Calibration IA Screen

D.   INPUT/OUTPUT CONNECTIONS

The I/O configuration for *AC100* and *America* are given in Table I. The module numbers given in Table II are entered by the user to the hardware connection editor to define the type of I/O device required.

Table I: I/O Configuration

Module	*America*	*AC100*
IP_Serial	3	1&3
IP_HiADC	1	-
IP_DAC	2	2
IP_68322	4	4

As an example, the HITL design project requires an IP_68322 I/O module for the PWM connection from the C30 to the AROD. The voltage signal from the AROD to the C30 uses the IP_HiADC module. Appendix A includes the HCE input and output screens for this project.

A brief description is given below for the I/O modules used in the avionics lab. References are also provided which contain more specific details on each module and procedures for making the required connections.

1.   Serial Connections/ IP_Serial Module

The IP_Serial module provides two channels of high performance multi-mode serial communication, [Ref. 6] section 5 page 69. Both RS-232-C and RS-422 are fully supported. The module can be programmed to baud rates of 2 Mbit/sec and asynchronous or synchronous protocols.

2.   Analog-to-Digital Connections/IP_HiADC

The HiADC provides 16 input analog channels with 12-bit resolution and synchronous sampling of all inputs, [Ref. 6] section 5 page 61. The module can convert one analog channel in 1.2 μsec or approximately 800 K samples/second. Each channel has a fixed voltage range of $\pm$ 5 V. No anti-aliasing filtering is provided for by the module so inputs should be band-limited to ½ the sampling frequency of the system.

3.   Digital-to-Analog Connections/IP_DAC

The DAC module provides six channels of 12-bit digital-to-analog conversion. Each channel can be configured to either $\pm$ 5V or 0-10V output ranges, [Ref. 6] section 5 page 34.

4.   Pulse Width Modulation Connections/IP_68332

The IP_68332 module is a time processing unit (TPU) that can perform one or more hardware I/O functions, [Ref. 6] section 5 page 52.   It can be programmed to generate various digital I/O signals, the current set-up in the avionics lab will use Pulse Width Modulation (PWM) signals. In the PWM mode, the user specifies the duty cycle as the output from the SystemBuild diagram.

V.   DIGITAL CONTROL DESIGN

The RealSim rapid prototyping series allows for control system to be tested in real-time with hardware-in-the-loop while recording any or all the state variables to verify performance. This section will step through the design process using a simple controller to control the control surfaces of the *FROG*.

A.   MODELING ACTUATORS AND SENSORS

Before the controller can be designed, a mathematical model of the plant which is to be controlled must first be created. The techniques involved to develop the model depend on the characteristics of the plant. This section details the technique used to model the actuators used on the *FROG*. Since both the *FROG* and AROD's control surfaces are actuated by Futaba FP S34 servo motors, the AROD is used in the lab.

To develop an accurate representation of the Futaba actuators, the system is modeled as a second-order transfer function.

$$H(s) = \frac{\omega_n^2}{s^2 + 2 \cdot \zeta \cdot \omega_n \cdot s + \omega_n^2}$$

The system response is obtained by applying a step function to the actuators and recording the response using the data acquisition editor feature of the RealSim software. To calculate the transfer function, the rise time t_r and maximum overshot M_p values are measured from the system response. From these values the natural frequency ω_n and the damping ratio ζ are calculated using the following formulae:

$$\zeta = \frac{\ln(M_p)}{\sqrt{\ln(M_p)^2 + \pi^2}} \qquad \text{(Eq. 5.1)}$$

$$\omega_n = \frac{-\tan^{-1}\left(\dfrac{\sqrt{1-\zeta^2}}{\zeta}\right)}{\sqrt{1-\zeta^2} \cdot t_r} \qquad\qquad \text{(Eq. 5.2)}$$

It is assumed the actuators have a rate-limiter therefore a small step response of 10 degrees is used so the effect of the rate-limiter on the rise time would be minimized. Then a larger step of 100 degrees is given to estimate the rate limits of the actuator. The results are plotted and shown in Figure 5.1 and 5.2. Note, to obtain a clearer picture of the actuators step response for the 10 degree step, the signal was fed through a lowpass filter with a cut-off frequency of 10 hertz.

From the 10 degree step response plot, values for the maximum overshoot M_p and rise time t_r were measured as:

$$M_p = .2 \qquad t_r = .06,$$

From equations 5.1 and 5.2, the ω_n and ζ were calculated as:

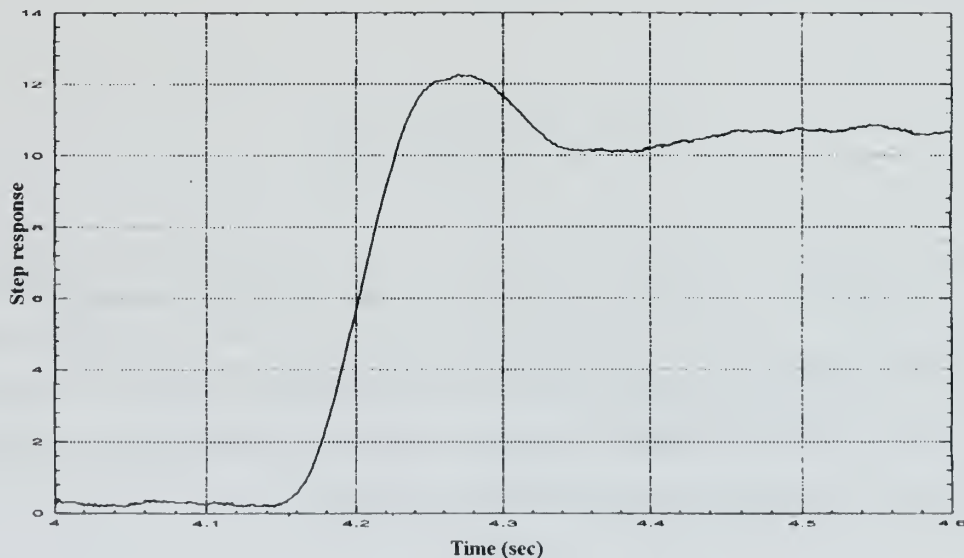$$\omega_n = 20.55 \qquad \zeta = .455,$$

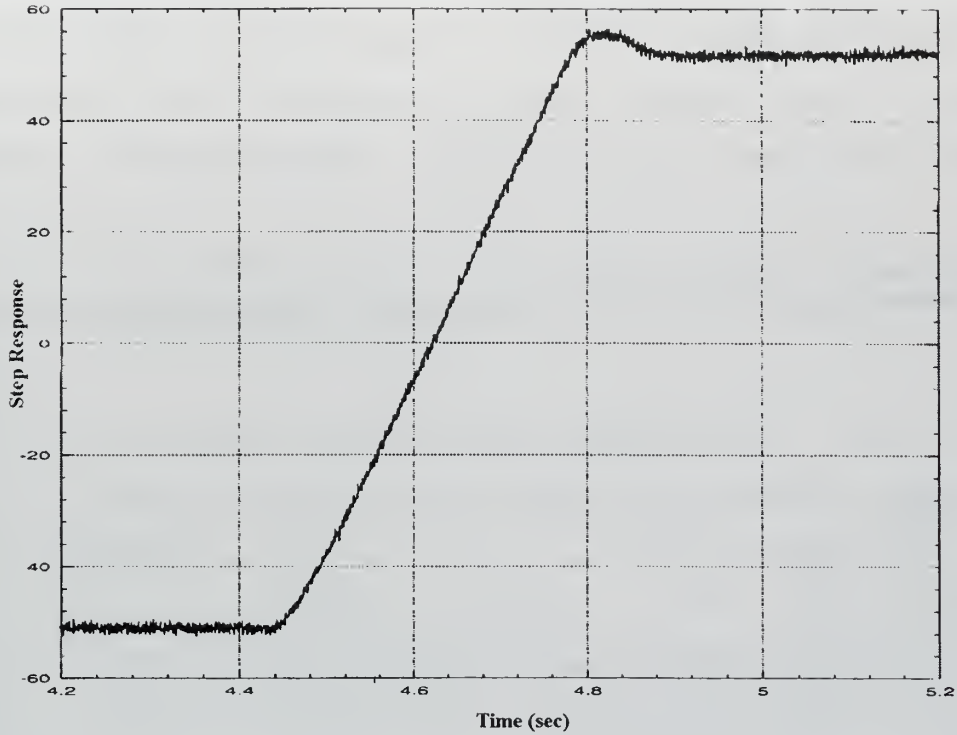**Figure 5.1: Step Response of Futaba Actuator (10 deg.)**

54

Figure 5.2: Step Response of Futaba Actuator (100 deg.)

The slope of the 100 degree step response is measured and used to calculate the rate-limiter, which was found to be approximately ±325 deg./sec.

The 2nd order transfer function can be given in general form by:

$$H(s) = \frac{a_1 s^{-1} + a_2 s^{-2}}{1 + b_1 s^{-1} + b_2 s^{-2}},$$

where

$$a_1 = 0$$
$$a_2 = \omega_n^{\ 2}$$
$$b_1 = 2 \cdot \zeta \cdot \omega_n$$
$$b_2 = \omega_n^{\ 2}$$

This transfer function was then implemented in SystemBuild, see Figure 5.3. Computer simulations were run on the model and the step response recorded and plotted along side the actuator's step response for analysis. By changing the damping ratio and natural

55

frequency of the transfer function, the step response of the model was made to match the response of the actuator. The final values for the damping ratio and the natural frequency were:

$$\zeta = .55$$
$$\omega_n = 25$$

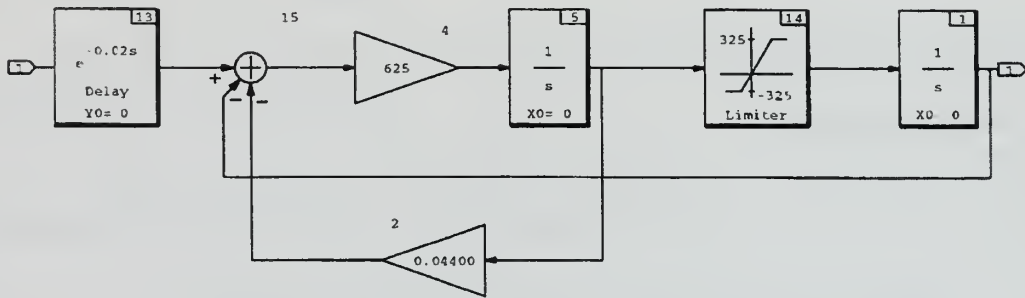The step responses of the final second-order model and the actuator are shown in Figure 5.4.
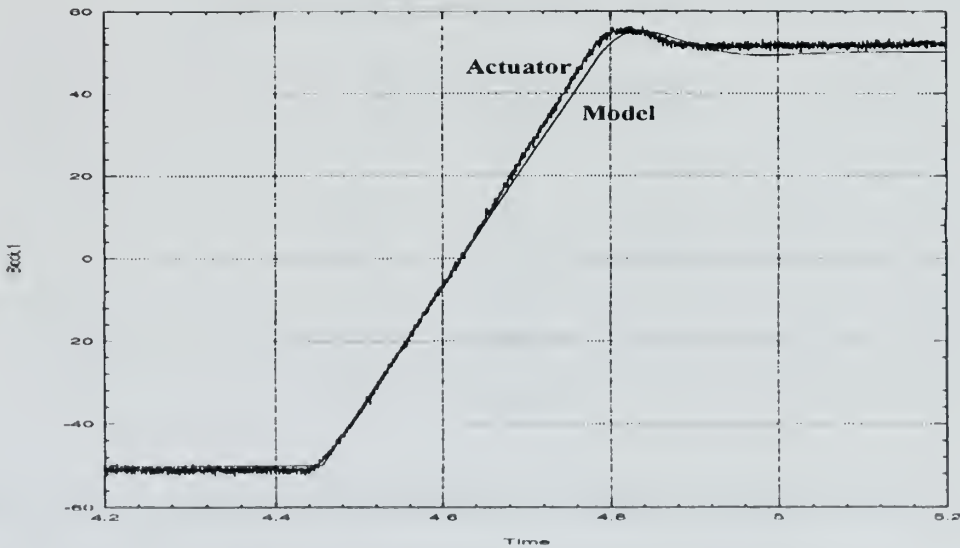

Figure 5.3: Second Order Actuator Model

Figure 5.4: Step Response of Actuator and Second-Order Model

56

B.   FEEDBACK CONTROLLER DESIGN

The next step is to design a feedback controller that satisfies specific requirements.   The requirements are normally specified in terms of response time, overshoot, stability and robustness. The controller design process is outlined below:

- Create a nonlinear model. A block diagram is formed that includes the plant model and nonlinear controller.

- Linearize the model and adjust controller gains.   The linear model is linearized and then analyzed using frequency response and/or root-locus methods.

- Analyze closed-loop system. Computer simulations are run with the feedback system, the controller gains are adjusted to create the desired control.

Applying classical control techniques, the controller model is generally first designed in continuous-time.   After a satisfactory response is achieved the system is transform to discrete-time and tested again for satisfactory response.

For this example the Speed_Controller developed in Chapter III is implemented with the actuator model. To analysis the system the loop between the controller and plant is broken as shown in Figure 5.5. The system is linearized using the Xmath command *sys=lin("SuperBlock name")*. The linearized model can be used to analyze the system using root-locus methods and Bode frequency response methods. The root-locus and Bode plots, shown in Figure 5.6, are generated using the Xmath commands: *rlocus(sys)* and *bode(sys)*. After a satisfactory response is obtained, the system is transformed to discrete-time and tested again.
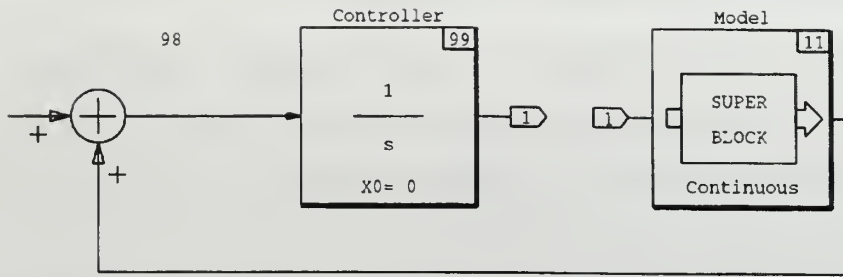
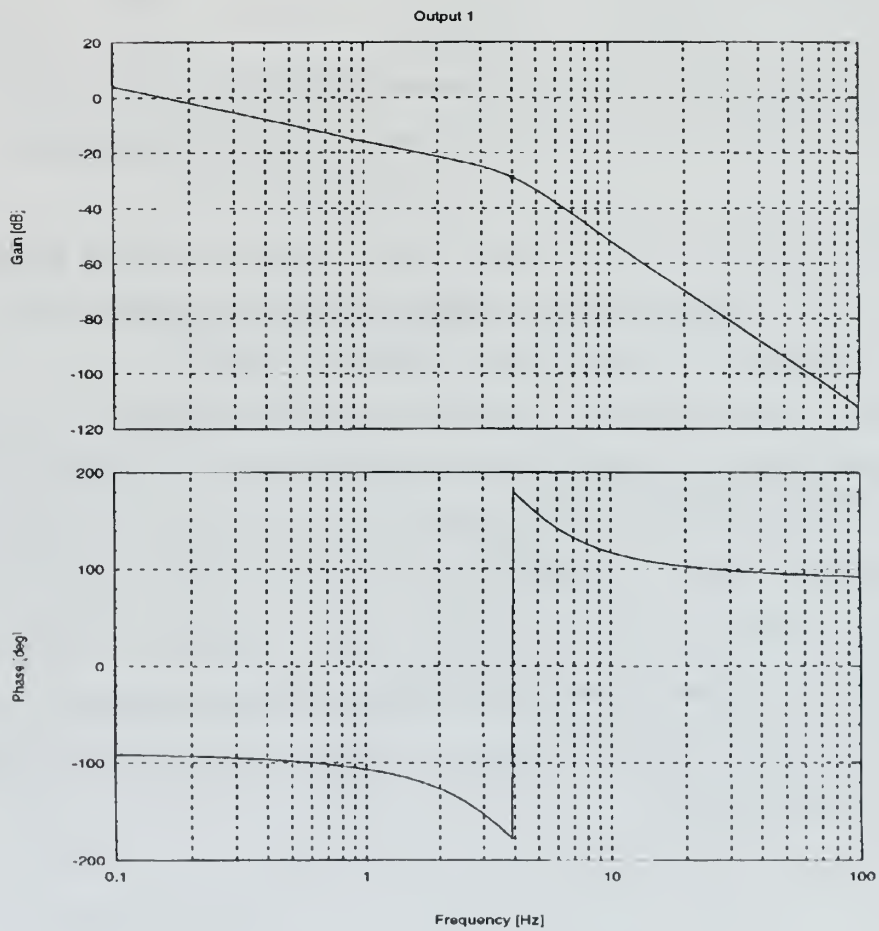**Figure 5.5: Broken-Loop Block Diagram**

Figure 5.6: Bode Plot

58

C.   HARDWARE-IN-THE-LOOP TESTING

Hardware-in-the-loop testing is where the feedback system is tested with some or all of the actual hardware. In this case, the design will include the actuator, the actuator model and the Speed_Controller, as shown in Figure 5.7.   This design allows the controller to be simulated with the actuator model or conduct HITL testing. If the actuator model is accurate and the controller design is correct, there should be no apparent difference in the performance of the controller. If the actuators are not modeled well, the test of the controller may indicate that the controller works as designed while the HITL test may show that the feedback system is unstable.
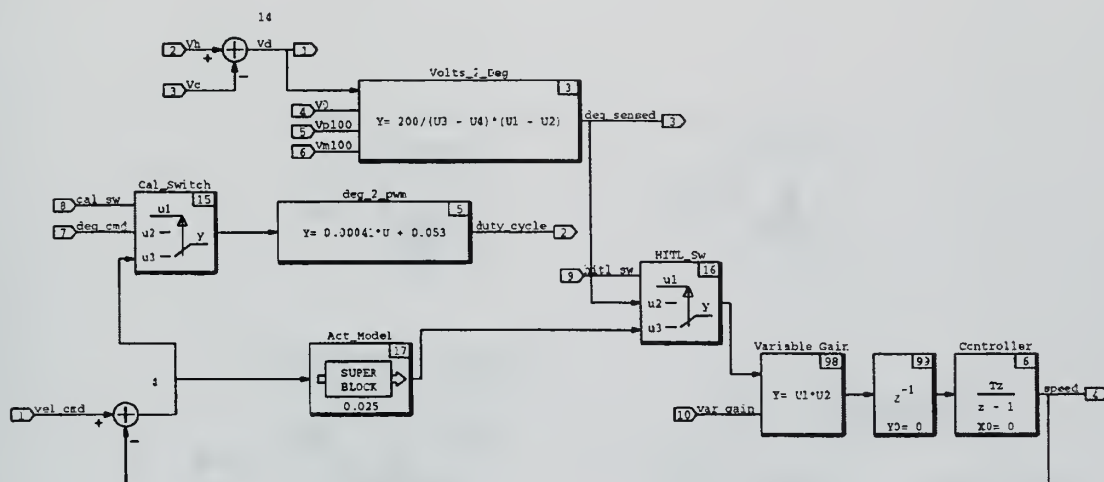

Figure 5.7: HITL Test SystemBuild Block Diagram

The simulation includes two switches for controlling the desired simulation state. The three simulation states are:

- Sensor calibration
- Actuator model
- HITL

The calibration switch controls which input command will be used by the actuators. With the calibration switch *On*, the command input *Deg_cmd* is used. When

the switch is *Off,* the commanded input is from the error signal of the *Vel_cmd* in the loop. The HITL switch will control which test is desired: the computer actuator model or the actual hardware. Table II summarizes these switch functions. The interactive animation page used to monitor and control the model is shown in Figure 5.8.

Table II: Simulation States

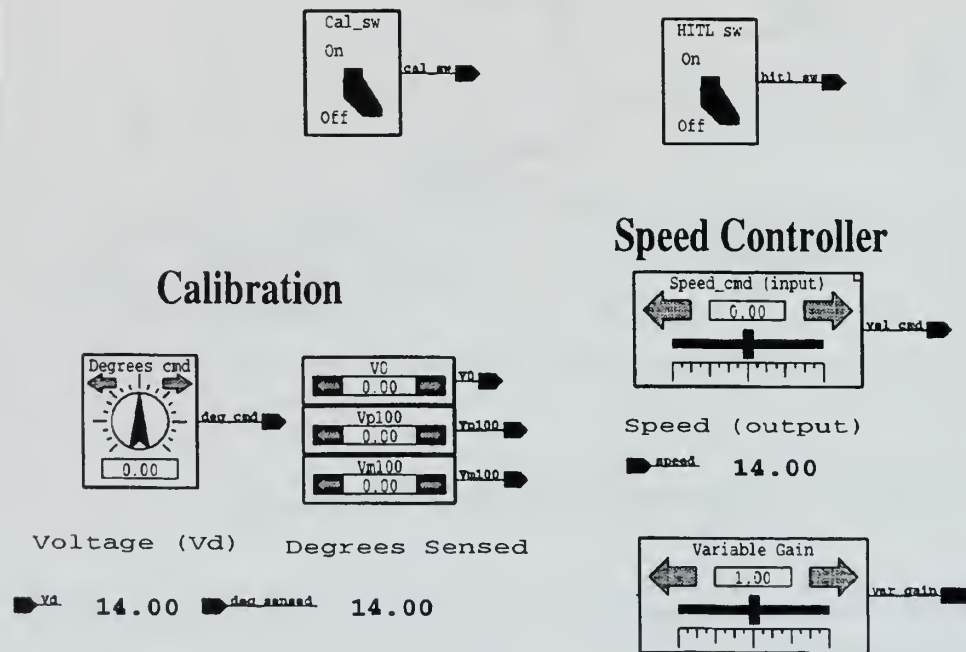| Calibration Switch	HITL Switch	Simulation
On	X	Sensor Calibration
Off	Off	Actuator Model
Off	On	HITL

Figure 5.8: IA Screen for HITL Test

The HITL design includes a variable gain block, which permits the user to adjust the gain during the testing. The gain margin can be found experimentally by running the HITL test and slowly increasing the gain until the system goes unstable. The results are

shown in Figure 5.9. The gain margin when determined experimentally is approximately 24 (-28db) which matches the gain margin found from the root-locus and bode plots.
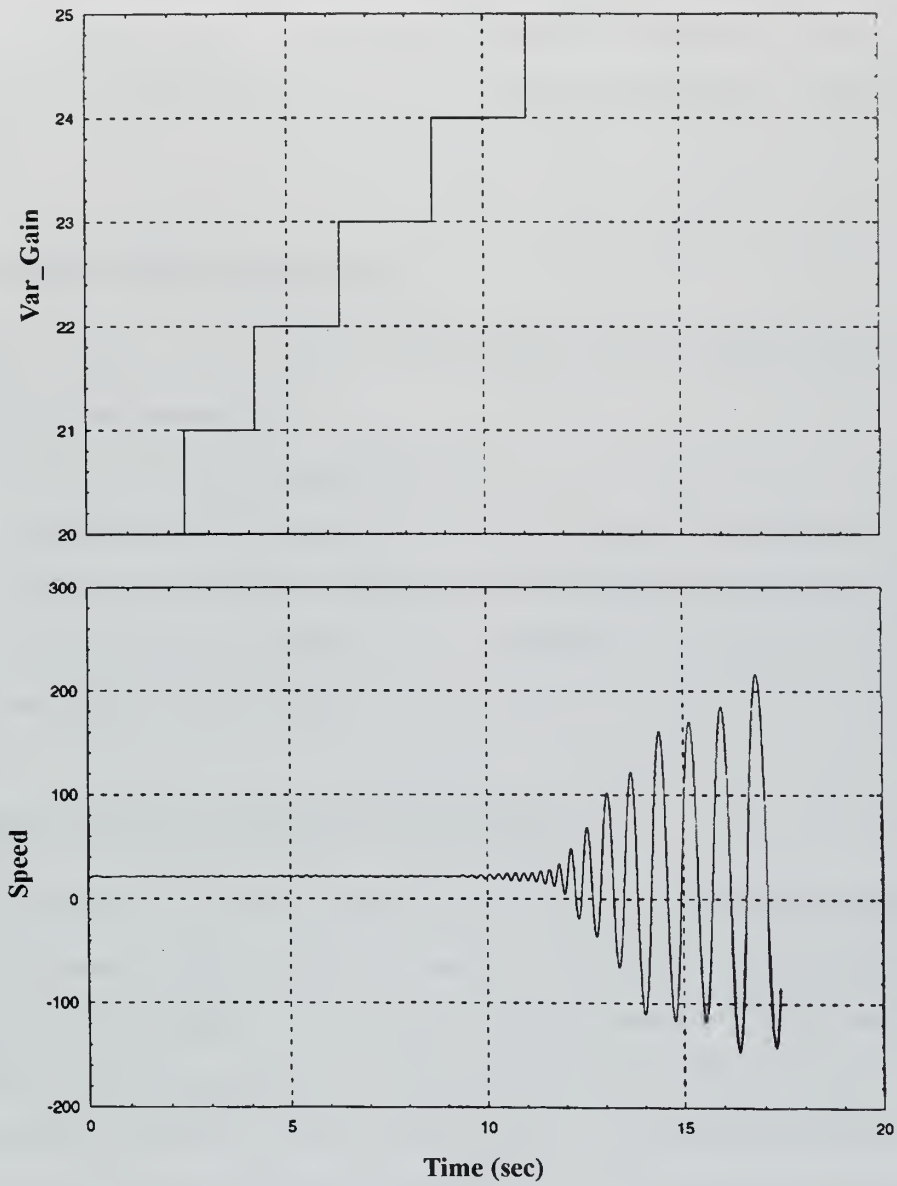

Figure 5.9: Gain Margin Results From HITL Test

VI.   ALTITUDE CONTROLLER DESIGN PROJECT

This chapter details the design and implementation of a digital controller utilizing the rapid prototyping system. Applying classical control techniques, the goal is to design a PI controller to be implemented on the UAV *FROG* that will track constant altitude in steady-state.

A.   DESIGN REQUIREMENTS

Design a PI controller for the combined model of the *FROG* and autopilot that satisfy the following requirements:

- The feedback system must be stable.
- The steady state tracking errors to constant altitude commands must be zero.
- The overshoot to step commands in altitude should not exceed 20%.
- The rise time in response to a step altitude command should be about 30 seconds for a 100 ft climb.

B.   *FROG* AND AUTOPILOT MODELS

The first step in the design process is to create a model of the aircraft. This model is developed from the equations of motion for the platform. A nonlinear model is first formed in a block diagram representation of these equations. The nonlinear model is then linearized about a desired trim point to create a linear model. There is also an autopilot installed in the *FROG* that must be modeled. The autopilot controls the elevator and aileron to command constant climb rate $\dot{h}_c$ and constant yaw rate r_c. The SystemBuild model for the combined *FROG* and autoplot was developed by a previous thesis student [Ref 7] and is shown in Figure 6.1, see Figure B.4 for the autopilot SuperBlock.

63

To determine the bandwidth available $\left|\dot{h}\middle/\dot{h}_c\right|$, the control bandwidth is first

determined. Figure 6.2 shows the −3db cutoff frequency equal to 2 rads/sec.
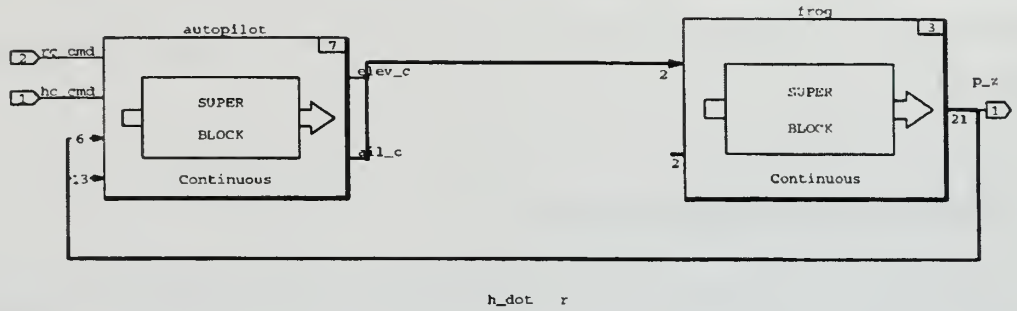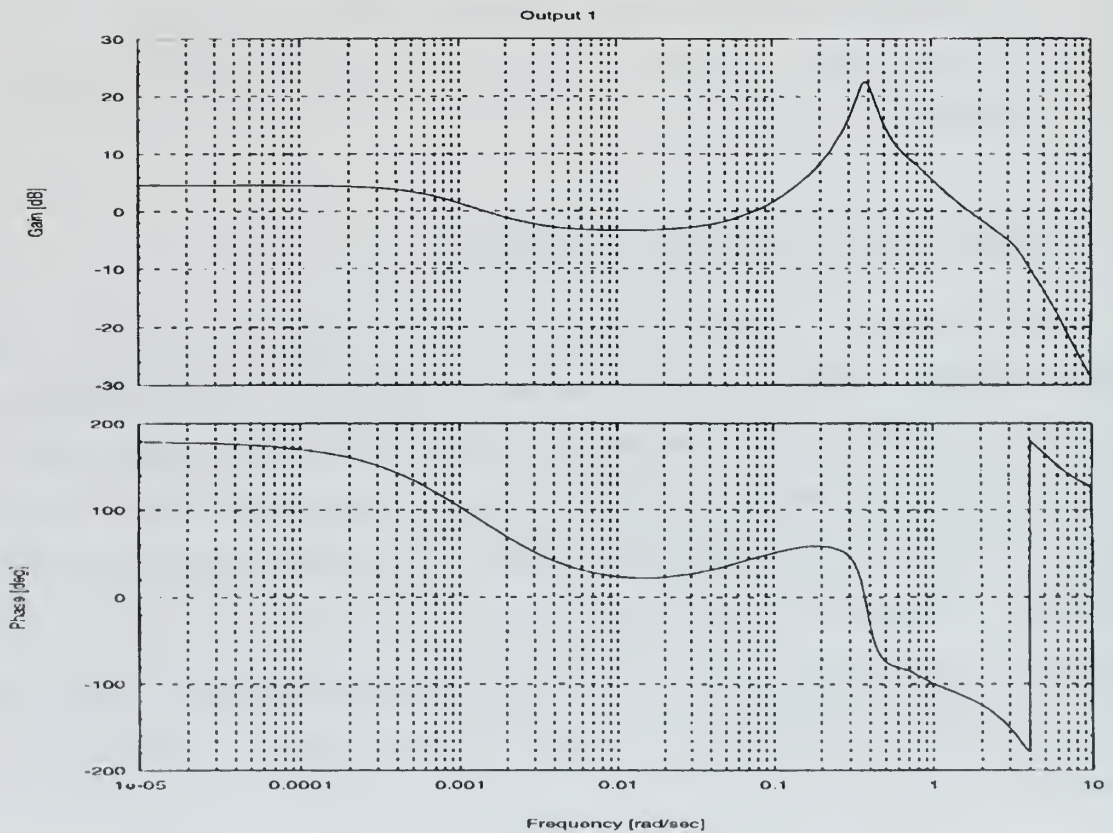

Figure 6.1: *FROG* **and Autopilot Models**

Figure 6.2: Elevator Control Bandwitdh

C. FEEDBACK CONTROLLER DESIGN

The next step is to design a PI controller that satisfies the requirements outlined in section A. This is an iterative process employing various methods with the controller gains being the design knobs used to meet requirements of response time, overshoot, and command and control loop bandwidths.

Applying classical control techniques, the initial controller gains are generally first obtained for continuous-time model. After a satisfactory response is achieved the system is transformed to discrete-time and tested again for satisfactory response.

1. Basic SystemBuild Model

The basic model is constructed with a PI controller and the complete *FROG,* autopilot, and actuator model developed in the previous chapter, and all known delays and nonlinearities. The known delays include: a transmission delay of 200 milli-second between the ground station and the *FROG*, and an update rate of approximately one second for the Global Positioning System (GPS) position. To model the GPS a ZOH function is developed using a discrete gain block with magnitude one and a sampling rate of $T = 1$ (sec). The complete system is shown in Figure 6.3.
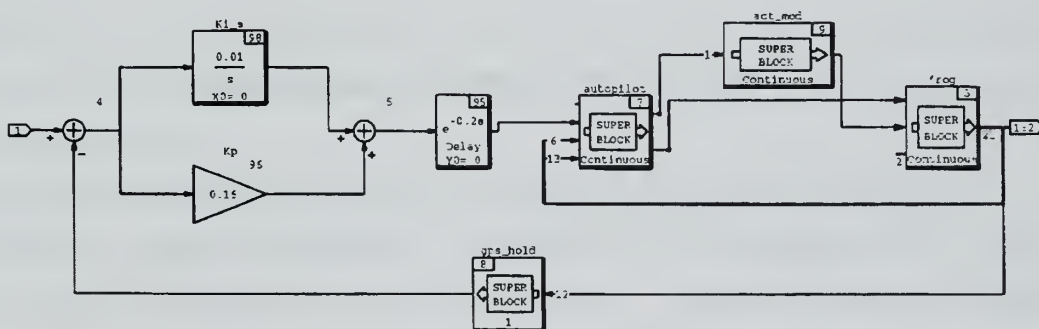

Figure 6.3: Basic SystemBuild Model for Altitude Controller

The following values of the PI controller gains were calculated to achieve the design requirements:

65

$$K_i = 0.01$$
$$K_p = 0.16$$

The basic system is simulated using Xmath, and the step response is shown in Figure 6.4.
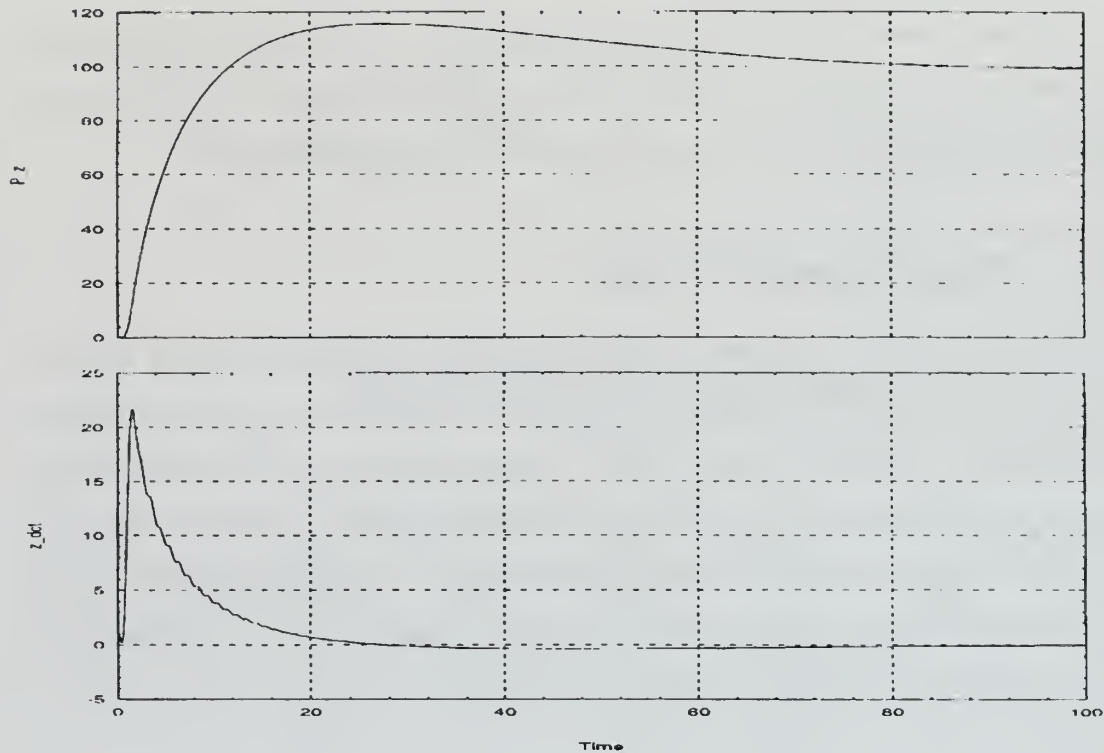
Figure 6.4: Step Response for Initial Design

A number of unsuccessful iterations were tried to reduce the overshoot of the step response while maintaining system stability. The nonlinear system is linearized as described in the next section. The linear model is then analyzed using root-locus methods and Bode frequency response. The analysis is demonstrated below.

Consider the system transfer function

$$\frac{h}{h_c}(s) = \frac{L(s)}{1 + L(s)} = \frac{(K_i/s + K_p) \cdot P(s)}{1 + (K_i/s + K_p) \cdot P(s)} \quad ,$$

where

$$L(s) = C(s) \cdot P(s)$$

This results in an extra zero in the numerator at $-K_i/K_p$, causing the overshoot. Therefore a second design was developed. The PI controller was modified, as shown in Figure 6.5.
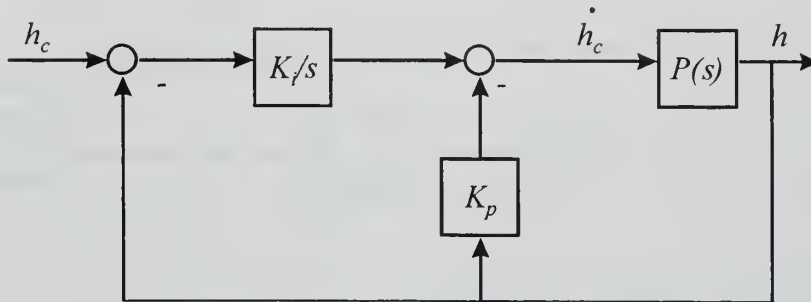
Figure 6.5: Modified PI Controller

Now the system transfer function is

$$\frac{h}{h_c} = \frac{K_i/s \cdot P(s)}{1 + \underbrace{\left(K_i/s + K_p\right) \cdot P(s)}_{L(s)}}$$

This system was implemented using delta implementation [Ref. 8], as shown in Figure 6.6. Note that SystemBuild does not have a differentiator block, therefore the following approximation is used:

$$s \rightarrow \frac{s}{\varepsilon s + 1} \quad , \quad \text{where } \varepsilon \ll 1$$

This design showed a significant reduction in the amount of overshoot. The system response is shown in Figure 6.7. The initial value for K_i produced a slower then desired response and was increased to .2 rads/sec. With a satisfactory step response observed in position and climb-rate, another simulation was run to check aircraft response to altitude commands, Figure 6.8.

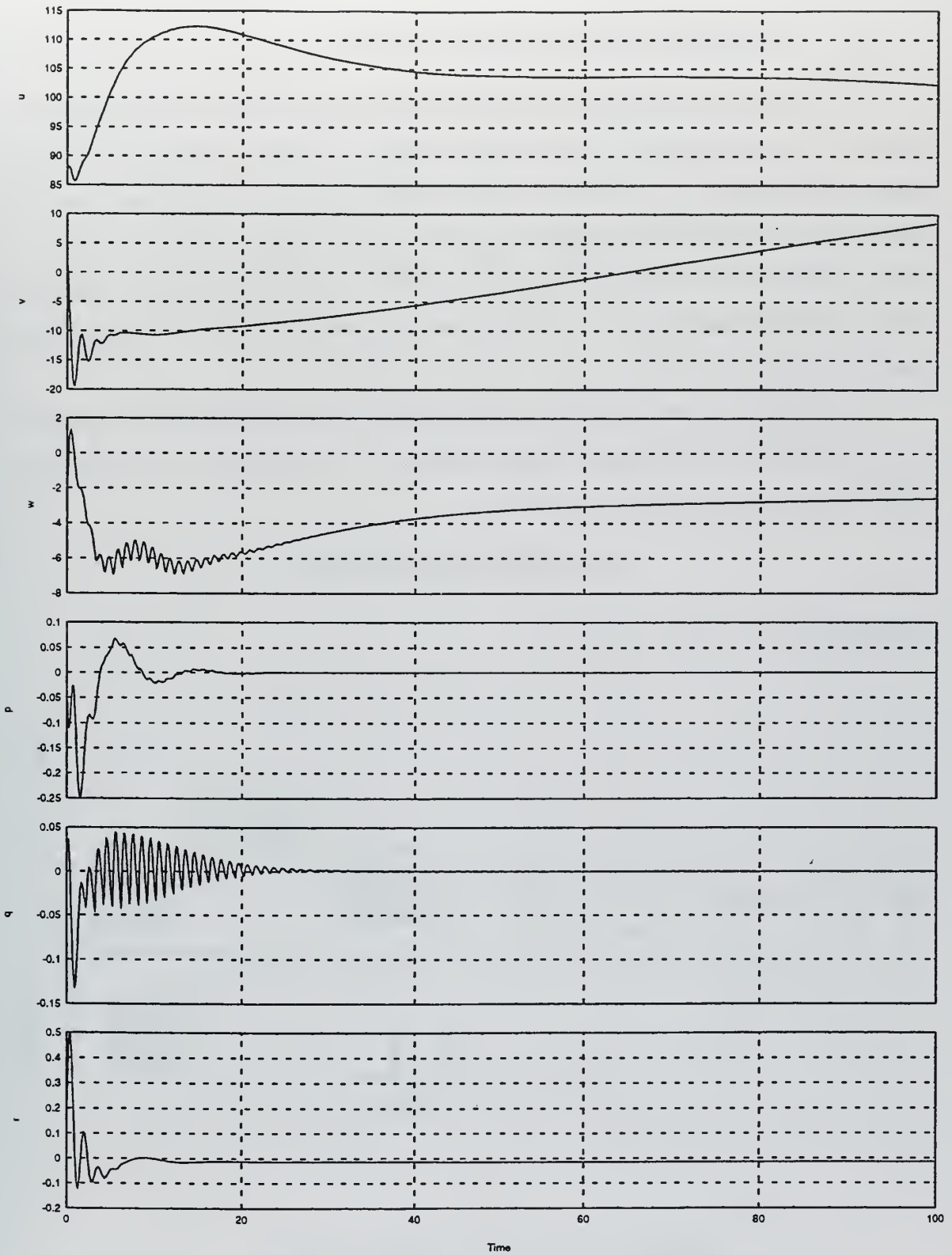**Figure 6.6: CTS Altitude Controller**

Figure 6.7: Step Response for PI Controller

Figure 6.8: Dynamic Response of Model

69

2.   Linearized Model: Further Analysis

To determine the stability margins of the system the root-locus and Bode analyses were done. The loop between the controller and plant was broken, Figure 6.9, and the system was linearized.   The interactive root-locus feature of Xmath was used to determine the location of the system poles and the gain margin.   The final results are shown in Figure 6.10, with a gain margin of –16db. The Bode plot was then generated and the command bandwidth of 0.2 rads/sec and the phase margin of 70 degrees were obtained, Figure 6.11.

The system was then discretized by transforming the SystemBuild block diagram. Note: delay blocks must be added to each integrator to avoid algebraic loop in RealSim. The differentiator approximation used here is:

$$s \rightarrow \left(\frac{Tz}{z-1} \right)^{-1} = \frac{1}{T} \cdot \left(1 - z^{-1} \right)$$
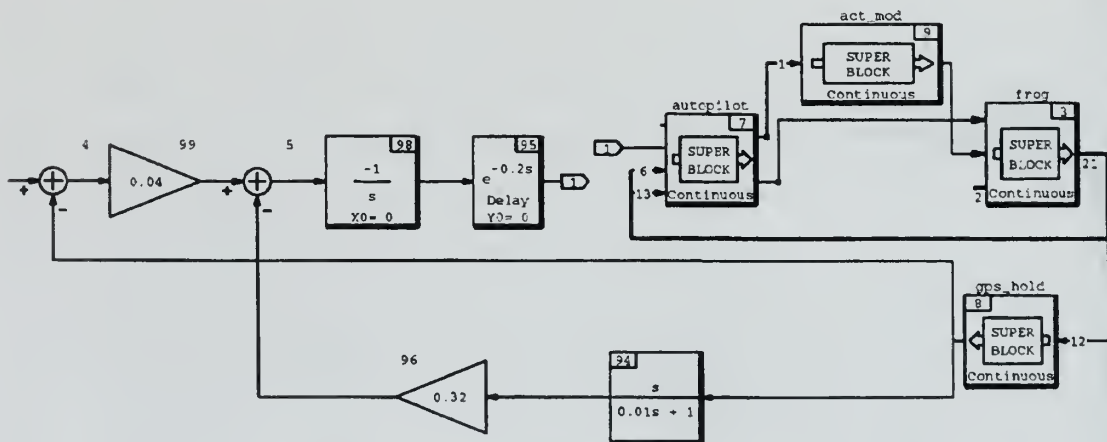
The discrete model is shown in Figure 6.12.

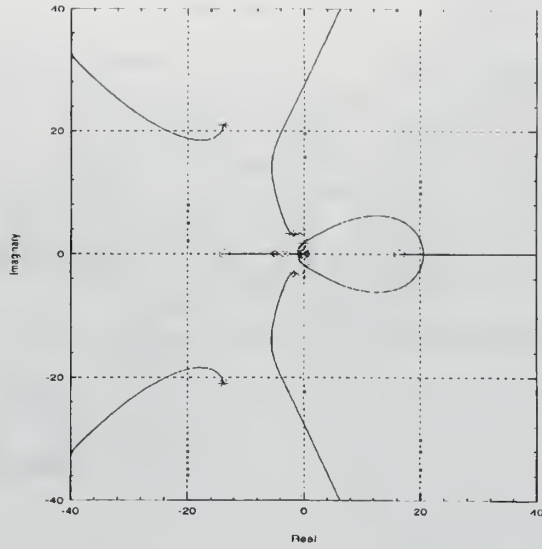**Figure 6.9: Broken Loop Block Diagram**

Figure 6.10: Root-Locus Plot
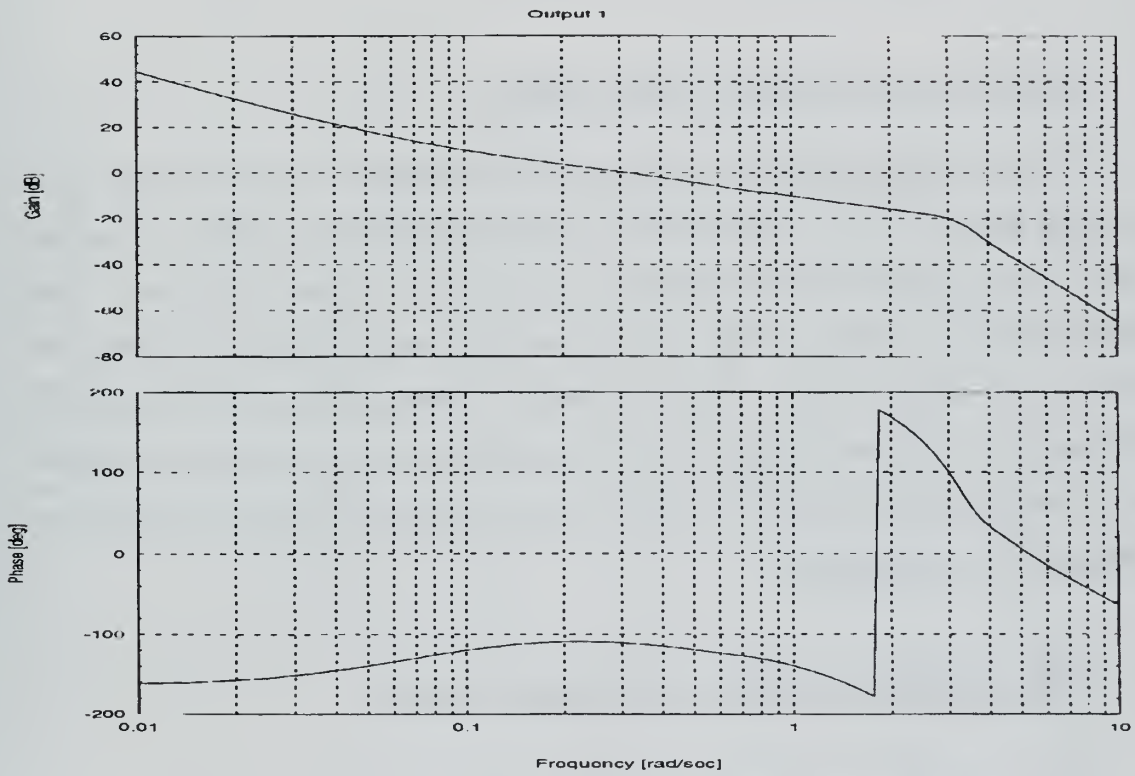
Figure 6.11: Bode Plot
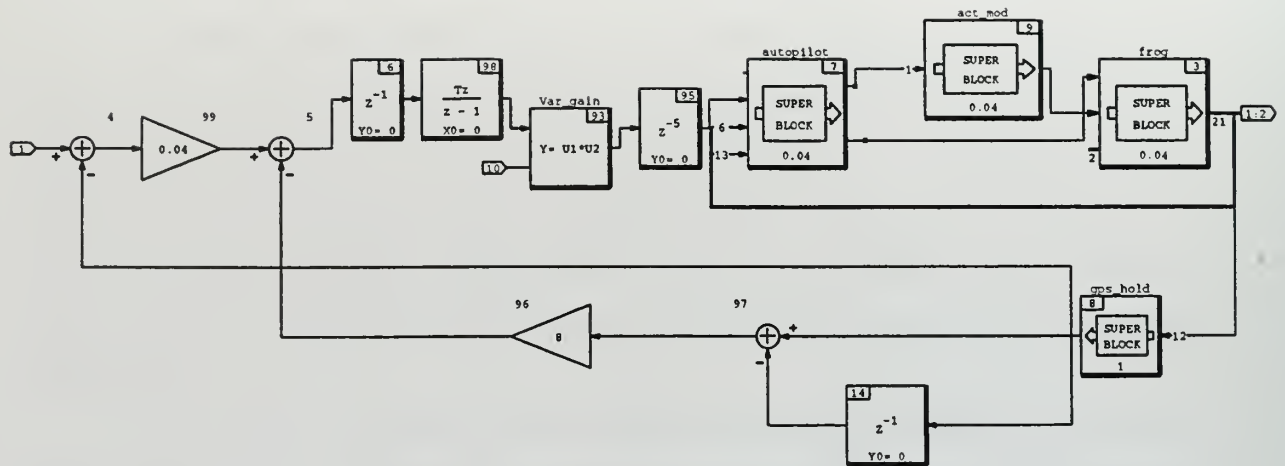
Figure 6.12: Discrete Altitude Controller Model

D. HARDWARE-IN-THE-LOOP TEST

The next step is a hardware-in-the-loop test. The actuators on the AROD set up in the avionics lab are the same actuators that control the elevator for the *FROG*. Therefore the HITL test can be conducted as described in the HITL section of this thesis. The necessary conversion blocks for the PWM output signal and voltage input signal were added to the controller design. Since the elevator command from the autoploit and *FROG* model is in radians, two more blocks were added to convert degrees and radians. The HITL SystemBuild model for the HITL testing is shown in Figure 6.13 and the test results are shown in Figure 6.14.

E. IMPLEMENTATION AND FLIGHT TEST

1. Implementation

The final step is to implement the controller into the flight management system for the *FROG*. This system manages a number of functions including navigation and flight control. The SuperBlock structure of the flight management system is separated

Figure 6.13: HITL Test Model For Altitude Controller

Figure 6.14: HITL Step Response For Altitude Controller

into five lower level SuperBlocks according to their function. The altitude controller is inserted into the control SuperBlock as shown in Figure 6.15. Appendix B contains the hierarchy for the SuperBlocks that make up the complete flight management system.

The UAV can be controlled by either the computer or RC pilot with a standard RC Futaba transmitter. A complete description of the *FROG* and its components is given in [Ref. 9]. To prevent large control inputs during transitions from RC pilot to computer control, the altitude controller is implemented using a delta altitude as the input command. As an example, if the user desired to maintain level altitude at hand off, a command of zero should be given. A script block is used to freeze the GPS altitude position at hand-over. The delta commanded altitude is then summed with the frozen altitude position and is used as the entered altitude command for the controller. The controller outputs a climb-rate command to the autopilot. The feedback loop uses the GPS altitude position referenced with respect to the local tangent plane (LTP) at the field. The orientation of the frame is specified as North-East-Down (NED), therefore a conversion gain is added to the feedback loop to reverse the sign. A conversion gain is also added to the controller's output. The *FROG* autopilot model differs from the actual autopilot in the units used for the entered climb-rate command. The model uses (ft/sec) where the actual autopilot uses (ft/min). The two switches are part of the wind down loop. If either or both switches are in the "OFF" position, the integrator is forced back to its initial value. This is done to prevent initiation of the controller at a previous state.

Once the controller is added to the flight management system, the user interface is added in the Interactive Animation screen used to monitor and control the *FROG*. The necessary input/output devices are added to the existing throttle control IA page, shown in Figure 6.16. For the initial flight testing, the screen is designed to display a number of performance variables not normally used for an operational flight display. These displays help evaluate whether the controller is working properly. The two digital output displays show the commanded altitude and the actual GPS altitude in feet. When the altitude controller is operating and working properly, the altitude readouts should match. An open loop input for the climb-rate is also added. With this feature the climb-rate command can be given directly to the autopilot by the user. The input slide gage is added

to adjust the gain during the test. The trainer light in the middle of the page indicates who is controlling the vehicle, the computer or the pilot.
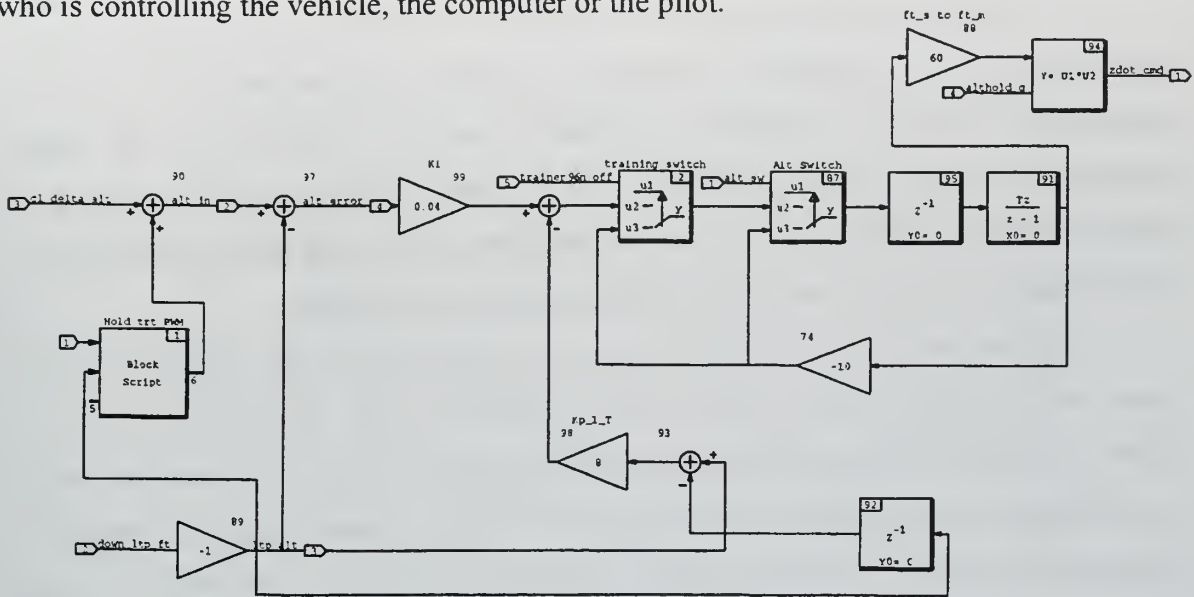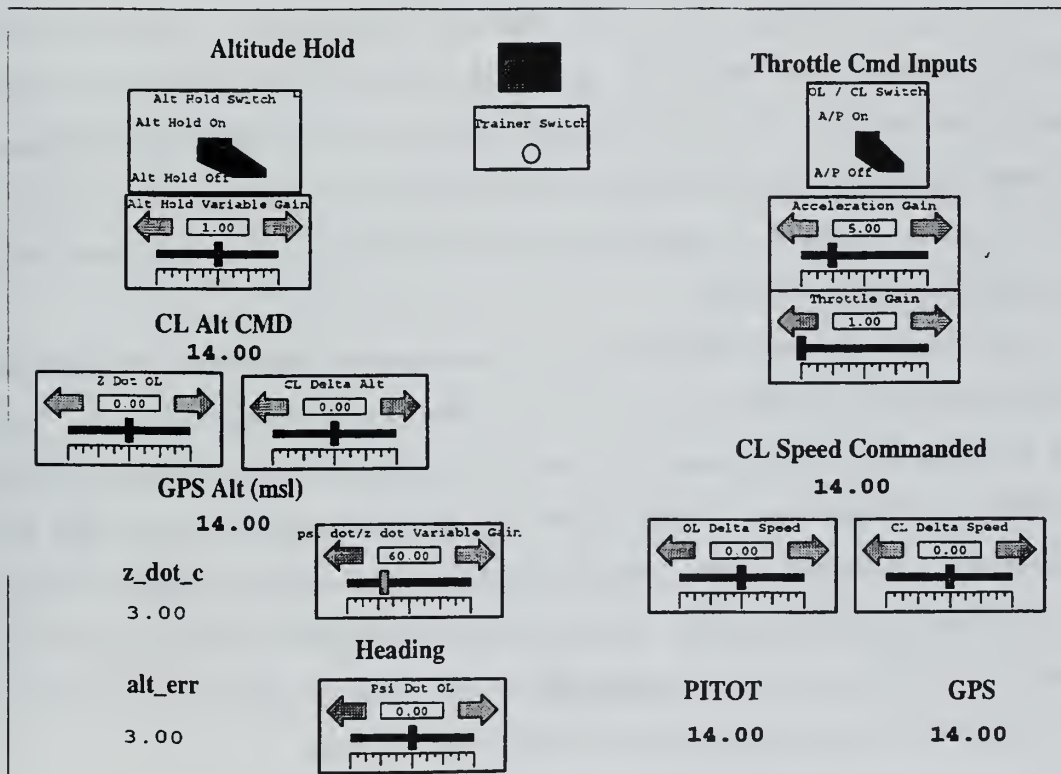

Figure 6.15: Altitude Controller SuperBlock

Figure 6.16: IA for Altitude Controller

2.   Flight Test

The flight test is conducted at a RC modelers club airfield located near the Naval Postgraduate School. The RPS is completely portable, and fits easily in a car for transport to the field. A flight plan is written a couple of days prior to the flight describing the conduct of the test flight. After all flight checks have been completed, a face-to-face pilot briefing is given to review the flight conduct and hand-off procedures. Normally the hand-off is accomplished during steady-state level fight.

Eight test runs were performed during two test flights. The data acquisition editor feature of the RealSim software was used to record the data. For each test run, the Airspeed Controller was used to maintain constant airspeed. The first three runs tested the performance of the Altitude Hold Controller in a turn. From the ground station, it appeared the controller maintained altitude within a ± 50 ft band. The next three runs tested the controller's performance in response to climb commands. A 100 ft climb command was given from a straight and level altitude. Each time the controller responded well to the climb commands and leveled off appropriately. Once level, the *FROG* seemed to be chasing altitude. From observation, it was concluded the controller was chasing altitude due to GPS drift. Secondly, the aircraft was making rapid changes in pitch intermittently due to the latency in GPS data, as seen in Figure 6.17. To reduce the pitch activity a filter (s/s+3) was added to filter GPS altitude. Two more runs were conducted with the filtered GPS data.

The test results for the controller in a turn are shown in Figure 6.17. The altitude error and commanded climb-rate from the controller show correct operation.   As expected, the drift in the GPS caused the controller to chase altitude. The data shows many gaps of 3-5 seconds with no GPS update. Figure 6.18 details the results from the climb commands. As designed, the controller climbed to altitude and smoothly leveled off. The commanded climb-rate was well within the aerodynamic limits of the *FROG* and appropriate for the climb. The performance of the controller with the filtered GPS, shown in Figure 6.19, was unstable with the errors slowly growing.

Overall, the Altitude Controller performed as designed. The commanded climb-rate in response to the altitude error is good. The shortfall is the GPS sensor.   Current plans include upgrading the *FROG's* pitot-static system. With a reliable altimeter used as

feedback instead of GPS, a substantial improvement in controller performance would result.
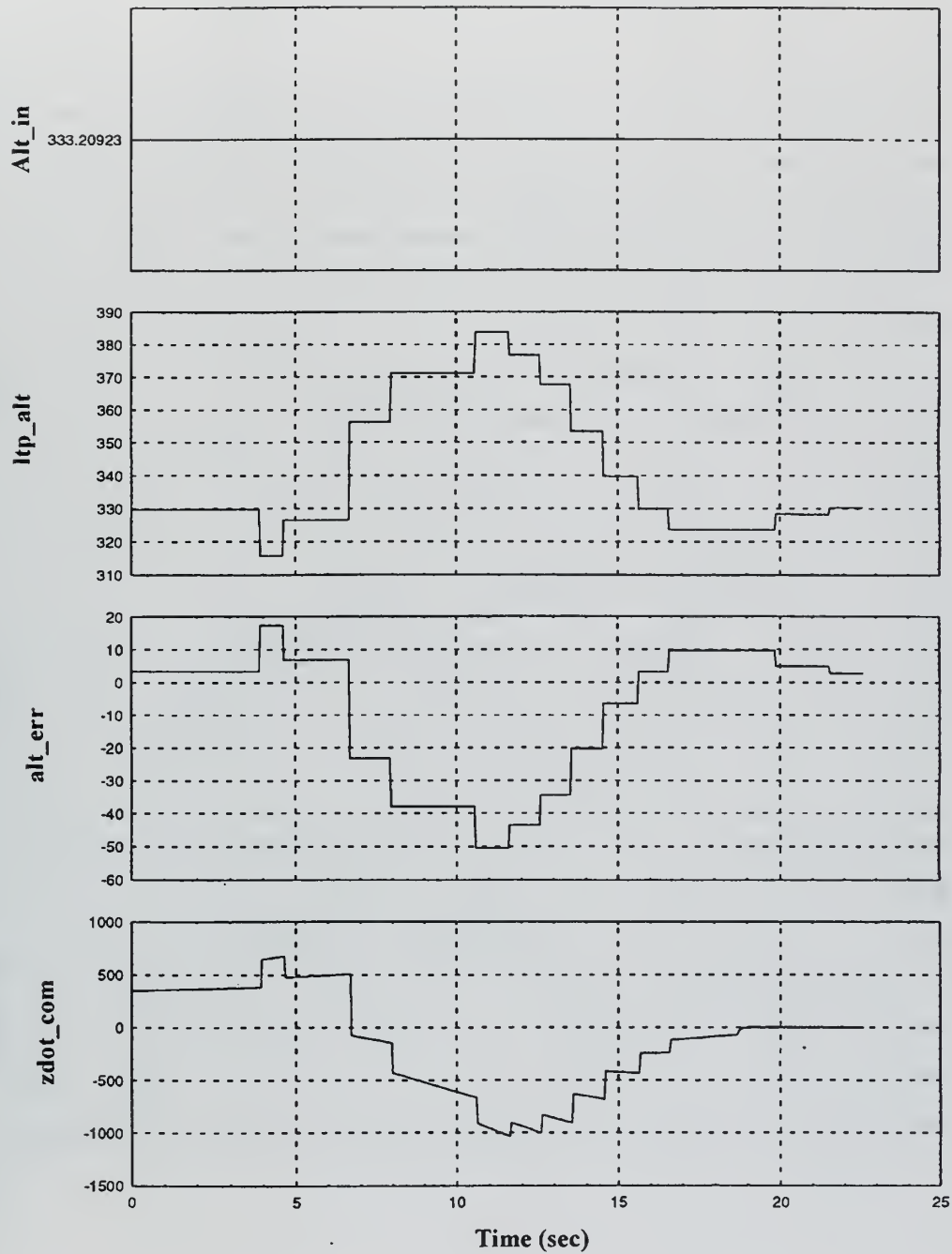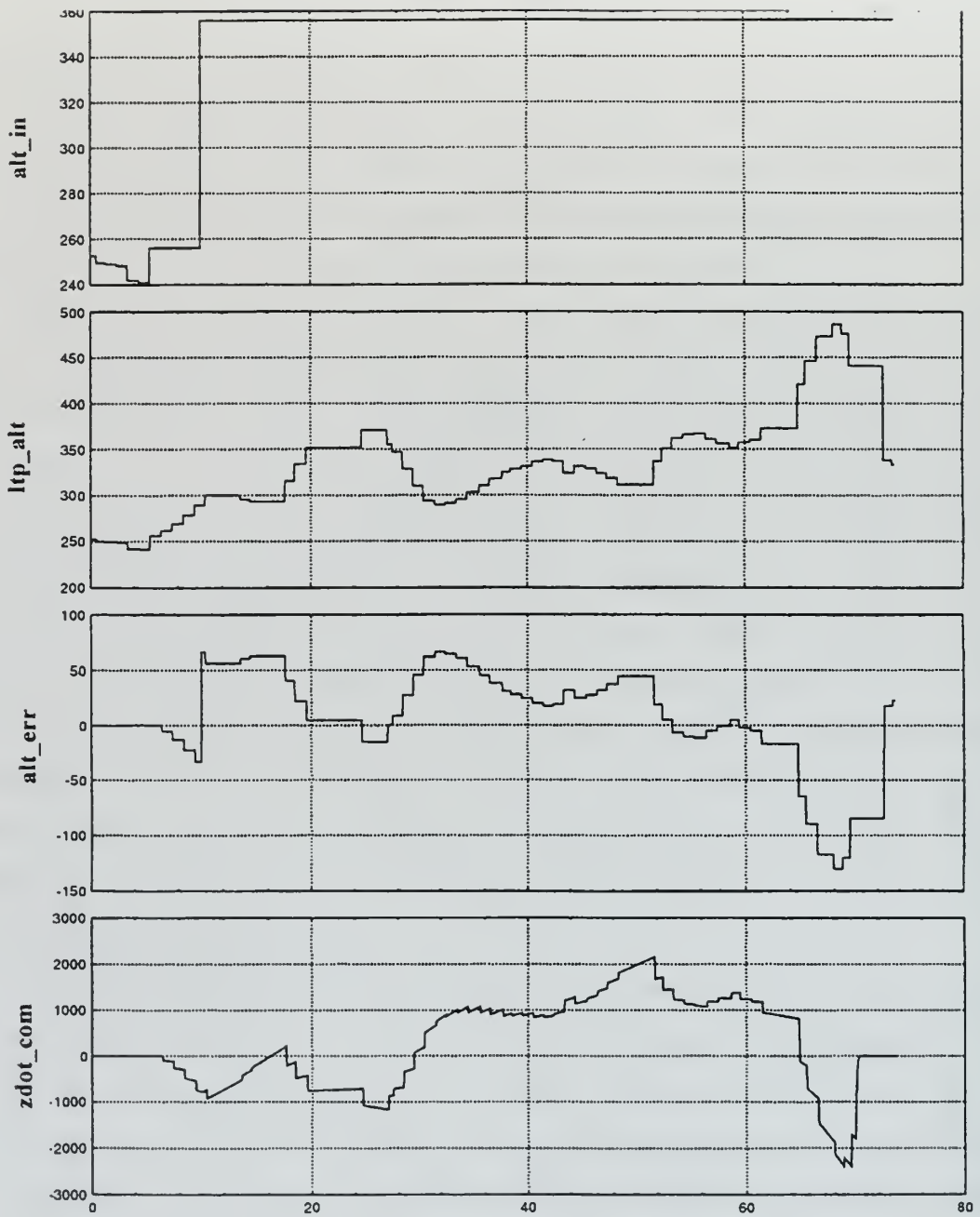
Figure 6.17: Flight Test Results for Turn

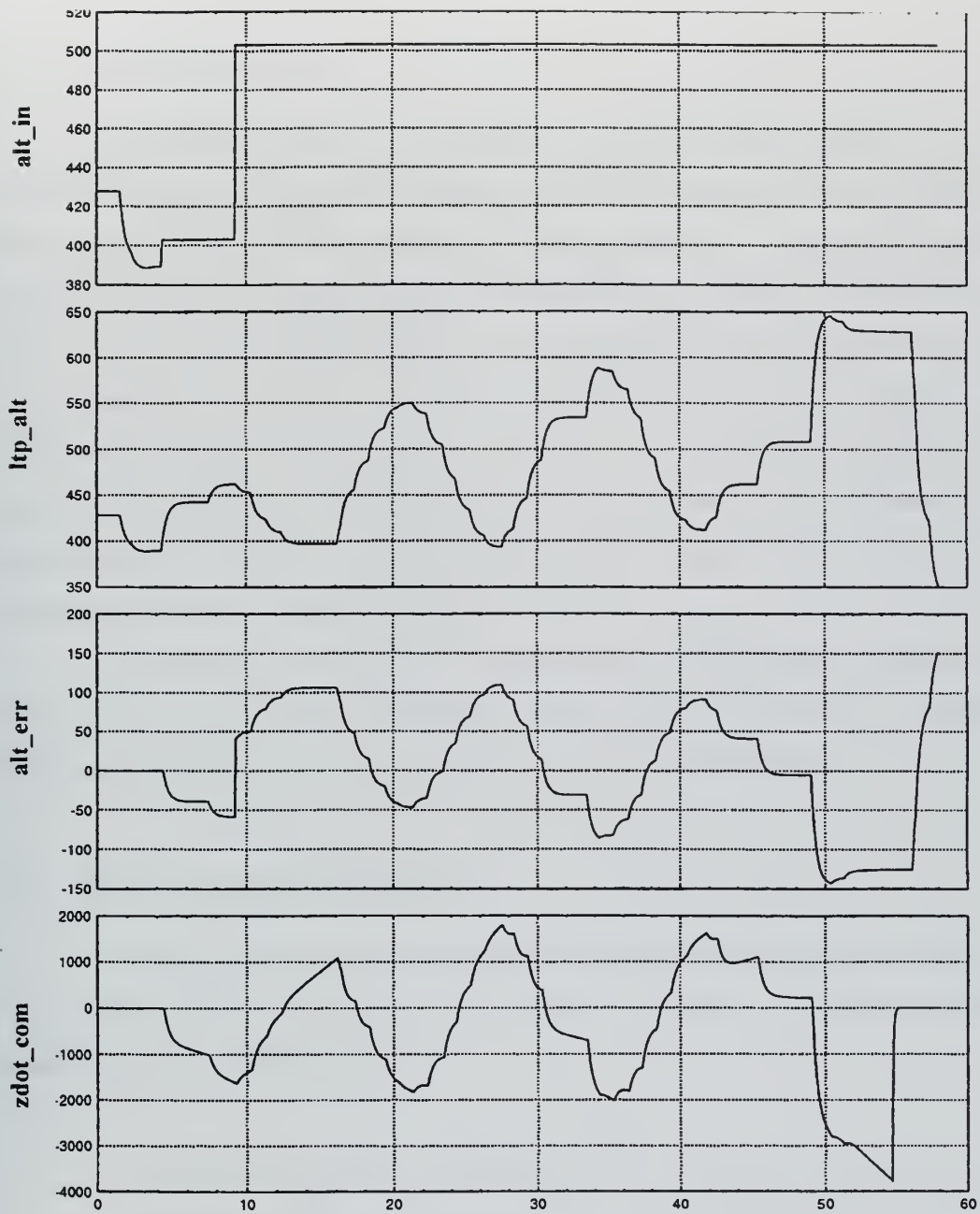**Figure 6.18: Flight Test Results for Climb**

78

Figure 6.19: Flight Test Results for Filtered GPS

VII. CONCLUSIONS AND RECOMMENATIONS

A.   CONCLUSIONS

The Advanced Controls of Aerospace Vehicles course, offered at the Naval Postgraduate School, provides an excellent opportunity for students to apply classical and modern control methods to the design of basic controllers.   A strong foundation is presented on the operations and analysis of sampled-data systems. The rapid prototyping system, developed by the department, is an excellent design tool and allows the student valuable hands-on experience in the design, implementation and flight testing of control algorithms for unmanned air vehicles. The ability of the application software, RealSim, to automatically generate higher-language code and eliminate the time consuming task of programming the code for a working model, enables design projects ample time to be completed in the twelve weeks allotted for the course.

Even though the RPS is still in its initial stages of development, it has generated a number of thesis opportunities, with many more foreseen in the future. Utilizing mostly off-the shelf technology, the cost of this educational tool will be minimal.

B.   RECOMMENDATIONS

Considering the conclusions stated above and the knowledge gained in the course of instruction given in the Advanced Controls of Aerospace Vehicles, the following recommendations are forwarded:

- Investigate scheduling this course, and its prerequisites, earlier in the avionics curriculum.   The UAV program developed by the department produces many excellent opportunities for thesis work. To allow ample time for students to complete their thesis work, this class should be scheduled prior to the last quarter of instruction.
- Presently there are no elective courses offered by the aeronautical engineering department in the area of digital control. Investigate the establishment of an

elective course that would introduce to the student system identification methods and advanced multivariable and optimal control procedures.

- Devote more classroom time to Design of Digital Control Systems Using Transform Techniques presented in Chapter V of [Ref. 1], and Design of Digital Control Systems Using State-Space Methods presented in Chapter VI of [Ref. 1]. Less time should be given to Chapter II of [Ref. 1], Linear, Discrete, Dynamic-Systems Analysis: The z-Transform. Material covered in chapter 2, discrete Fourier transform (DFT), z-transform, and block diagram descriptions, should be introduced during the prerequisite course, EO 2402, Introduction to Linear Systems.

- Establish a library within the avionics lab containing all previous thesis work and material related to the UAV *FROG*. Many of the design projects and future thesis work will build on the work from past projects. Good documentation is required to keep track of modifications, input/output variables, and improvements made to the system.

- Purchase a second target computer to supplement *America*. Currently the computer lab has only one computer with the AC100 model set-up and often two or three students end up waiting for access to *America* to compile and link their programs or to run the hardware setup.

APPENDIX A: HCE SCREENS FOR HITL PROJECT


```
┌─────┐  Use left mouse button, tab, shift-tab, or return to select items.
│Hints│  Use middle mouse button on toggle items for pull-down menu's.
└─────┘

<-- SB INPUT -->  <--------- DEVICE --------->  <------- ATTRIBUTES ---------->
chan label(1:10)  type            '     mod ch# initial_value final_value

1    vel_cmd    MONITOR_INPUT     0   0   0                    0
2    Vh         IP_HiADC          1   1   0                    0
3    Vc         IP_HiADC          1   2   0                    0
4    V0         MONITOR_INPUT     0   0   0                    0
5    Vp100      MONITOR_INPUT     0   0   0                    0
6    Vm100      MONITOR_INPUT     0   0   0                    0
7    deg_cmd    MONITOR_INPUT     0   0   0                    0
8               NO_DEVICE         0   0   0                    0
9               NO_DEVICE         0   0   0                    0
10              NO_DEVICE         0   0   0                    0


    Device_Type          Module          Channel_Number
    MONITOR_INPUT           0                   0

Initial_Value........ : 0.
Minimum_Value........ : -1.0E+37      Maximum_Value......... : 1.0E+37
Offset............... : 0.           Scale_Factor......... : 1.
SbHwInputToUserClient.. : disconnected SbInputFromUserClient.. : connected

┌──────┐                                                        ┌──────┐
│CANCEL│   Grouping       Viewing_Attributes    Selection_Mode  │ DONE │
└──────┘   by_SB_channel  initial_and_final_values    single    └──────┘
```

Figure A.1: HCE Input Screen

```
┌──────┐  Use left mouse button, tab, shift-tab, or return to select items.
│ Hints│  Use middle mouse button on toggle items for pull-down menu's.
└──────┘
```

```
<-- SB OUTPUT ->  <--------- DEVICE --------->  <------- ATTRIBUTES ---------->
chan label(1:10)  type              mod ch# initial_value final_value

1    vel_out      NO_DEVICE          0   0    0              0
2    duty_cycle   IP_68332_PWM       4   1    0              0
3    deg_gen      NO_DEVICE          0   0    0              0
4    Vd           NO_DEVICE          0   0    0              0
5                 NO_DEVICE          0   0    0              0
6                 NO_DEVICE          0   0    0              0
7                 NO_DEVICE          0   0    0              0
8                 NO_DEVICE          0   0    0              0
9                 NO_DEVICE          0   0    0              0
10                NO_DEVICE          0   0    0              0
```

```
        Device_Type            Module          Channel_Number
        NO_DEVICE                0                   0

Initial_Value......... : 0.            Final_Value........... : 0.
Minimum_Value......... : -1.0E+37      Maximum_Value......... : 1.0E+37
Offset................ : 0.            Scale_Factor.......... : 1.
SbOutputToUserClient... : connected
```

```
┌────────┐                                                      ┌──────┐
│ CANCEL │   Grouping      Viewing_Attributes    Selection_Mode │ DONE │
└────────┘   by_SB_channel  initial_and_final_values   single   └──────┘
```
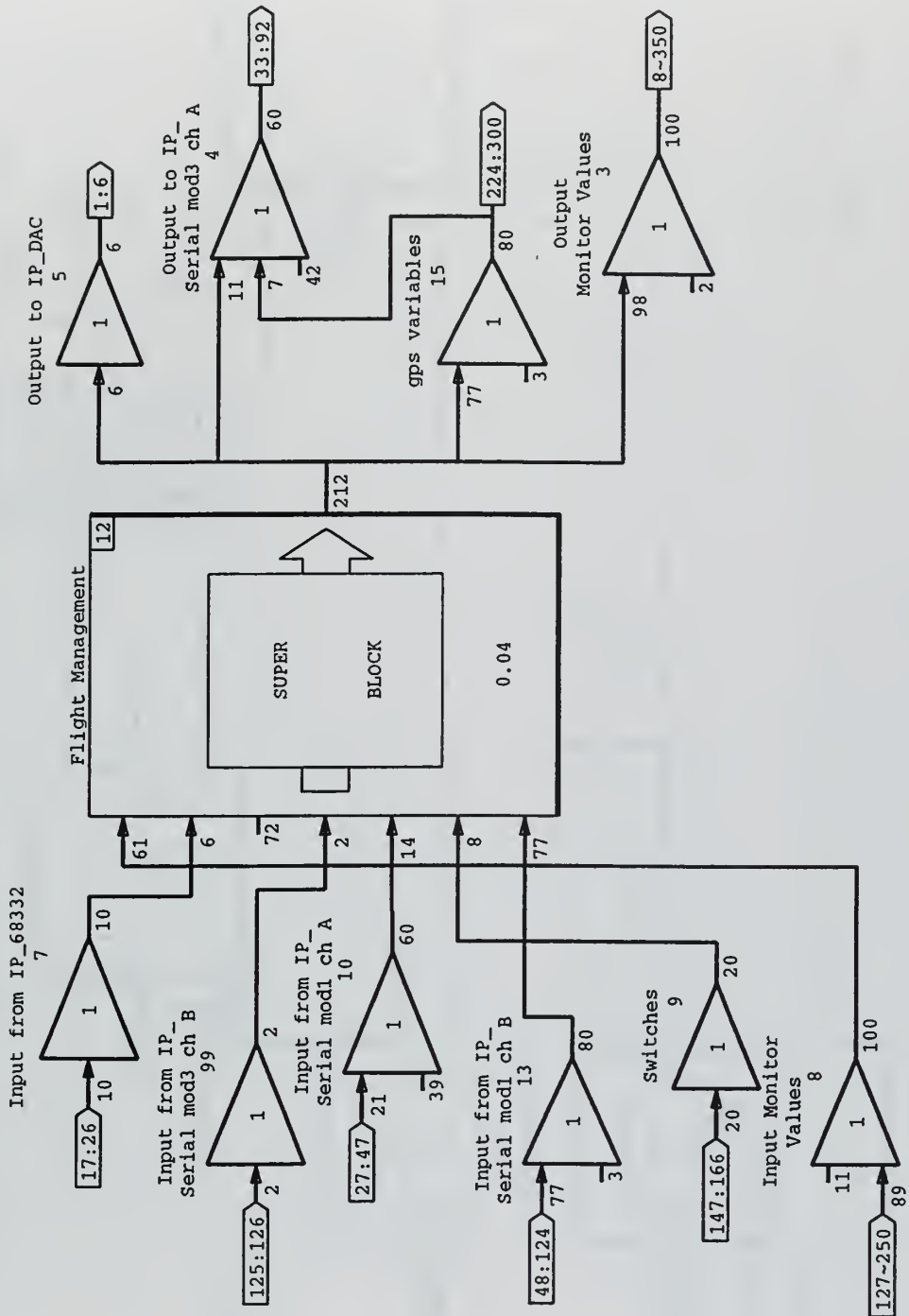
Figure A.2: HCE Output Screen
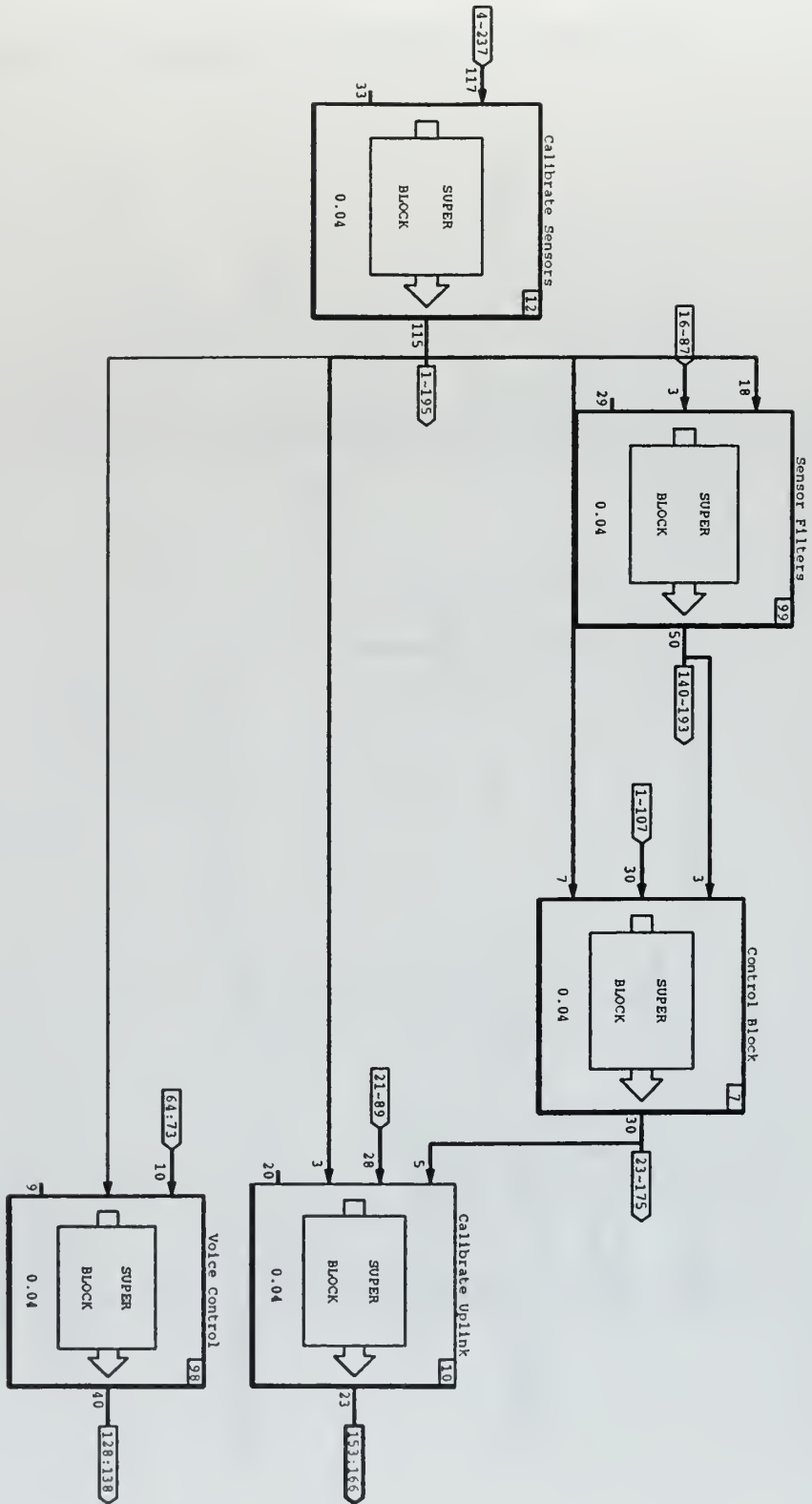
84

Figure B.1: Flight Test SuperBlock
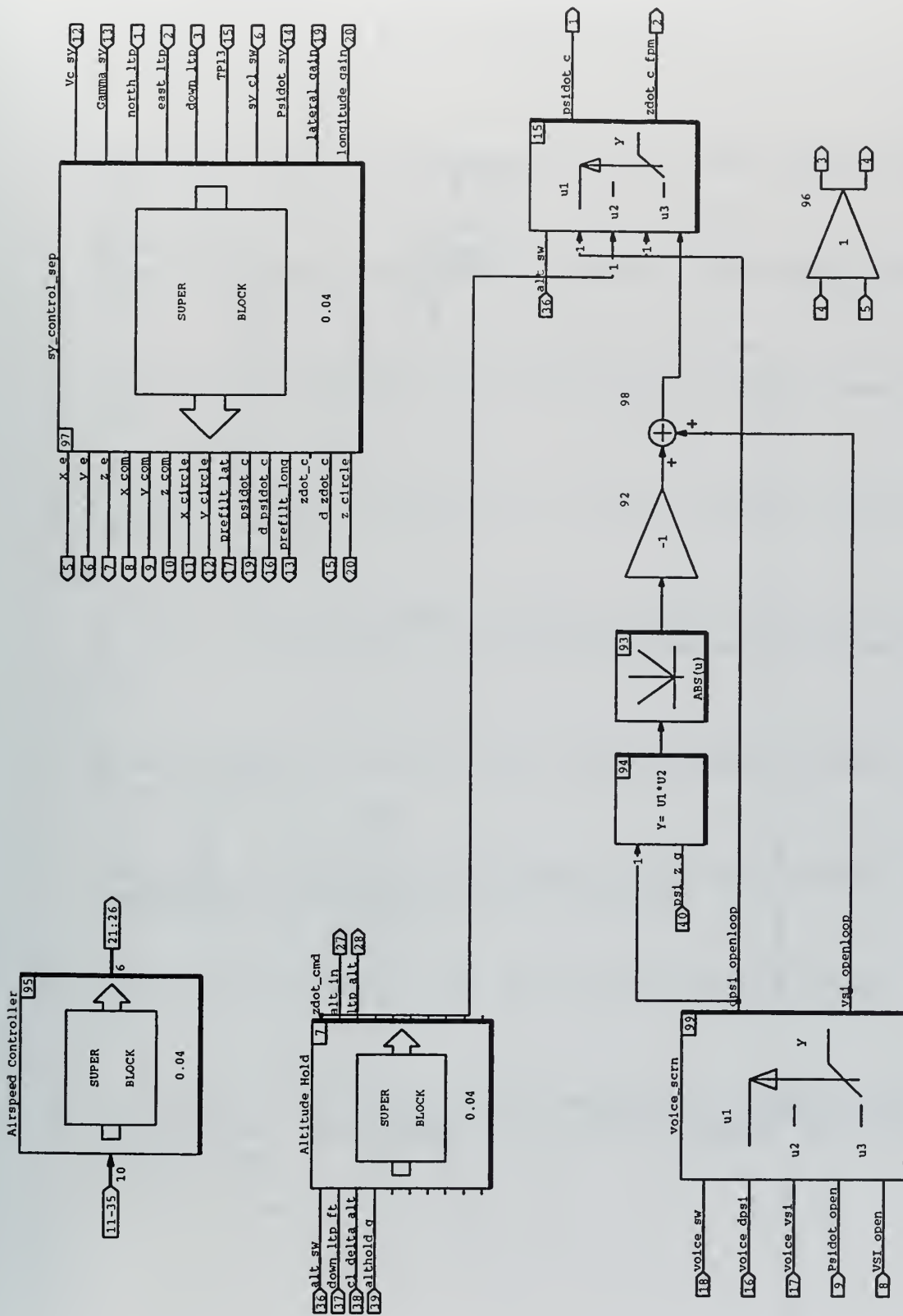
Figure B.2: Flight Management SuperBlock

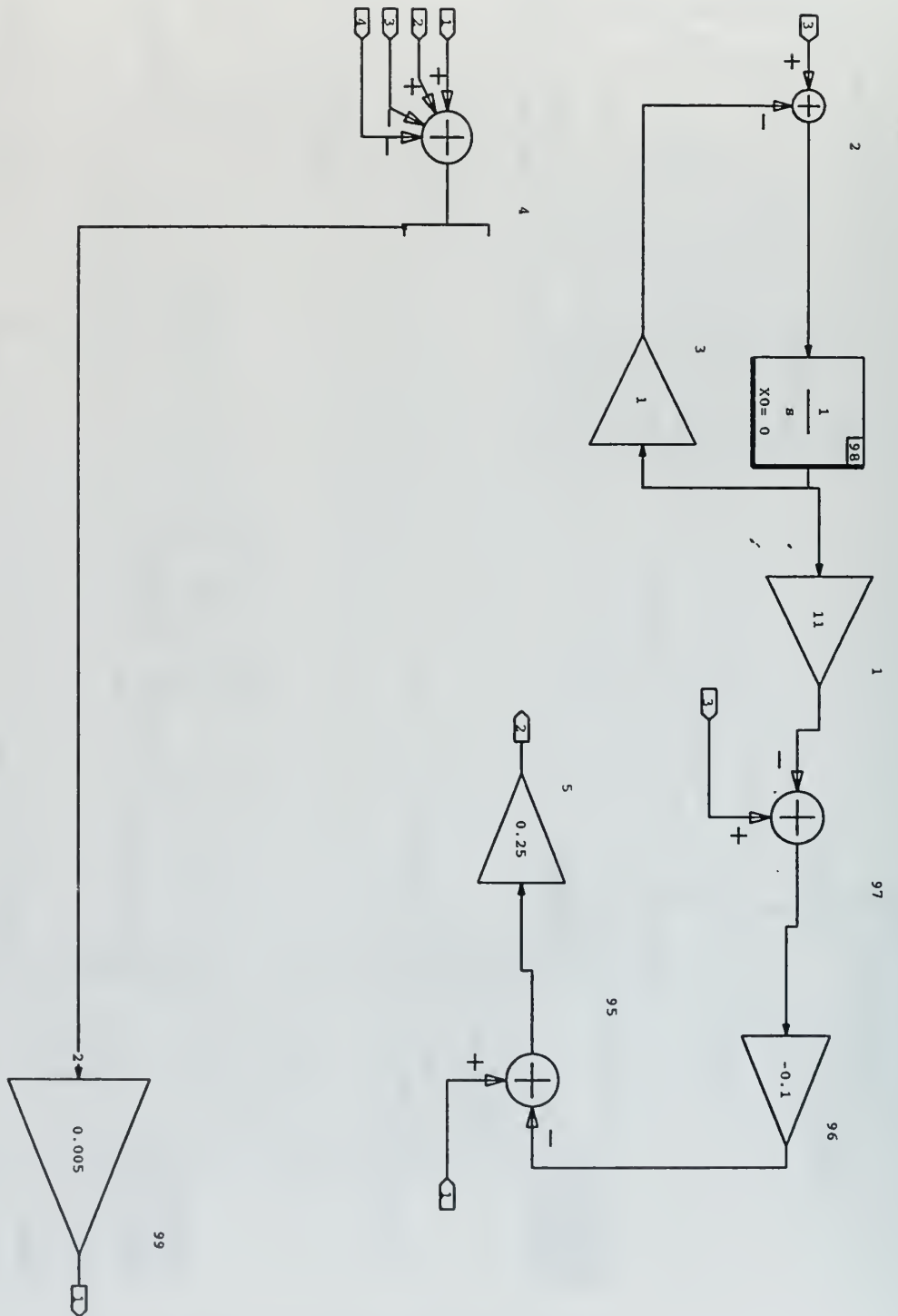**Figure B.3: Control Block SuperBlock**

Figure B.4: *FROG* Auotpilot Model

LIST OF REFERENCES

1. Franklin, G. F., Powell, J. D., Workman, M. L., *Digital Control of Dynamic Systems,* Addison-Wesley, 1990.

2. Strum, R. D., Kirk, D. E., *Contemporary Linear Systems,* PWS Publishing Company, 1996.

3. Kaminer, I. I., *Class Notes for AA4342,* Naval Postgraduate School, Monterey, CA, 1997.

4. Integrated Systems Inc., *MATRIX$_x$ Product Family System Manuals, SystemBuild,* Version 5.0, 1996.

5. Moats, M. L., *Automation of Hardware-in-the-Loop Testing of Control Systems for Unmanned Air Vehicles,* Master's Thesis, Naval Postgraduate School, Monterey, CA, 1994.

6. Integrated Systems Inc., *MATRIX$_x$ Product Family System Manuals, RealSim,* Version 5.0, 1996.

7. Papageorgiou, E. C., *Development of a Dynamic Model for a UAV,* Master's Thesis, Naval Postgraduate School, Monterey, CA, March 1997.

8. Pascoal, A., *Class Notes for AA 3341,* Naval Postgraduate School, Monterey, CA, 1997.

9. Komlosy III, J. A., *Applications of Rapid Prototyping to the Design and Testing of UAV Fight Control Systems,* Master's Thesis. Naval Postgraduate School, Monterey, CA, March 1998.

INITIAL DISTRIBUTION LIST

1. Defense Technical Information Center...2
    8725 John J. Kingman Rd., STE 0944
    Ft. Belvoir, Virginia 22060-6218

2. Dudley Knox Library..2
    Naval Postgraduate School
    411 Dyer Rd.
    Monterey, California 93943-5101

3. Doctor Isaac I. Kaminer, Code AA/KA...3
    Department of Aeronautics and Astronautics
    Naval Postgraduate School
    Monterey, California 93943-5121

4. Doctor Russel W. Duren, Code AA/DR..1
    Department of Aeronautics and Astronautics
    Naval Postgraduate School
    Monterey, California 93943-5121

5. Department of Aeronautics and Astronautics...1
    Code AA
    Naval Postgraduate School
    699 Dyer Rd. Rm. 137
    Monterey, California 93943-5106

6. LCDR Steven J. Froncillo...3
    712 Country Club BLVD.
    Chesapeake, Virginia 23460